University of Minnesota
ST. ANTHONY FALLS HYDRAULIC LABORATORY

Project Report No. 169

HYDRAULIC MODEL STUDIES OF THE CIRCULATING WATER SYSTEM FOR THE SHERBURNE COUNTY GENERATING PLANT - UNITS 3 AND 4

by

John F. Ripken
and
Todd Mendell

Sponsored by

NORTHERN STATES POWER COMPANY
Minneapolis, Minnesota

Plant Design by

BLACK & VEATCH, CONSULTING ENGINEERS
Kansas City, Missouri

January 1978
Minneapolis, Minnesota

TABLE OF CONTENTS

TABLE OF CONTENTS (Cont'd.)

ABSTRACT

The Sherburne Generating Plant of the Northern States Power Company is located 40 miles NW of Minneapolis. Plant Units 1 and 2 were placed in service in 1976 and 1977. Proposed Units 3 and 4 of 800 Mw capacity each were scheduled for commercial operation in the early 1980's.

Proposed design improvements in the circulating cooling water systems for Units 3 and 4 involved complex hydraulic flows. To assure performance, hydraulic model studies were undertaken. This report details the studies of a 1:12 model which were made at the St. Anthony Falls Hydraulic Laboratory.

In normal operations, heated water from the condensers is elevated to the top of forced draft cooling towers where it is released to spray downward for cooling. Start-up during sub freezing weather could lead to damaging freeze-up in the cooling tower. An added 84 inch diameter temporary cold weather by-pass drops the 168,000 gpm flow a distance of over 40 feet and requires a dispersed manifold port system assuring good energy dissipation and a stable, well-distributed flow into the tower basin. Based on initial model studies, several small changes were made in the original design to achieve the desired flow quality.

Flow in the cooling system is maintained by two 5,000 HP pumps drawing from a pump basin supplied by two cooling towers. The basin serves to route flow from either or both towers to either or both pumps. There was a concern that flow asymmetries or vortices detrimental to pump performance might be generated in the pump basin. Extensive tests at the model pump suction using pitots and vortex sensors establish that good flow conditions existed for all routings and no modification of the basin design was needed.

Separate considerations were given to the influence of trash screens and fire water pumping and the dispersion of additive acid in the pump basin.

LIST OF ILLUSTRATIONS

LIST OF ILLUSTRATIONS (Cont'd.)

HYDRAULIC MODEL STUDIES
OF THE
CIRCULATING WATER SYSTEM
FOR THE
SHERBURNE COUNTY GENERATING PLANT - UNITS 3 AND 4

I. Introduction

The Sherburne County Generating Plant of the Northern States Power Company is located near Becker, Minnesota. The plant is about 40 miles northwest of Minneapolis and adjacent to the Mississippi River. Plant Units 1 and 2, which are each of 680-Mw capacity, were placed in service in 1976 and 1977. Proposed Units 3 and 4, which are to be of 800-Mw capacity each, are to be placed in service in the early 1980's.

The design of all four units was by Black and Veatch, Consulting Engineers of Kansas City, Missouri.

The plant employs a circulating water system for condenser and auxiliary equipment cooling. In these systems heat transferred from the power plant condensers to the cooling water is conveyed by pumping the water through evaporative mechanical-draft cooling towers for heat release to the atmosphere. Make-up water is pumped from the Mississippi River. Operating experience with the recirculating water systems of Units 1 and 2 suggested the need for some modification and change before proceeding with the final plans for Units 3 and 4. The proposed new layout of one of the two twin cooling water circuits is shown in Fig. 1. The items considered in need of clarifying hydraulic model studies are shown in Fig. 1 as ; (a) the recirculating by-pass, (b) the cooling basin sump, and (c) the pump basin or sump for the main circulating pumps.

In the report which follows, the problems relating to the above system components are described together with the one-twelfth hydraulic scale model studies which are employed to define the operational characteristics of these components. The clarifying tests are then reviewed and recommendations made

II. The Recirculating Bypass - Its Function and Problems

As shown in Figs. 1-5, the low level 120 inch and 96 inch pressurized lines convey hot water from the plant condensers to a particular cooling tower. At the cooling tower these low level lines reduce to an 84 inch

diameter in rising to supply the distribution piping at the top of the tower. Following the vertical lift, the normal route of the recirculating hot water is through an 84 inch horizontal header pipe branching to two horizontal 60 inch valved distribution pipes and, thence, to drip-spray drainage vertically downward through the tower lattice work to collection in the cooling tower basin. However, when a system is started up during subfreezing weather, the system water may be in a near freezing state. As a result, ice may rapidly form on the exposed tower lattice work with a progressive weight increase which could lead to structural failure of the lattice system. To circumvent this possibility it was proposed to initiate cold weather start-up with the 60 inch distribution valves closed and the 84 inch by-pass butterfly valve open. Recirculation of the cold system water would then be maintained through the by-pass and directly to the cooling tower basin until adequate heat build-up had occurred in the water conveyed from the condenser. At this time the 60 inch tower distribution valves would be opened and the 84-inch by-pass valve would be closed to allow normal recirculation and drip-spray cooling in the tower.

Adoption of the vertical by-pass pipe provided means for maintaining workable temperature conditions in the water and the provision of free venting at the top of the pipe minimized the possibility of build-up of major start-up surge transients at the circulating pumps. However, the temporary introduction of the vertical by-pass into the flow routing also introduced a need for incorporating a new flow energy dissipator in the route before releasing the water to the cooling tower basin. Without such a dissipator major flow disturbances would be generated in the basin. Energy dissipation is needed because the system pumps lift the water about 43 feet above the tower basin to provide the head loss normally consumed in maintaining the drip-spray flow through the tower lattice works. (The pump energy required to provide the 43 foot lift with a design discharge of 126,000 gpm is approximately 1,400 horsepower.) During by-pass operation this excess horsepower in the water of the high-level header must be dissipated or dispersed before the water enters the low-level cooling basin.

The proposed by-pass design as shown in Fig. 2 intended that the accelerating dropshaft action in the vertical pipe; the abrupt flow expansion within the interior of the horizontal manifold; and the subsequent re-acceleration and expansion in the exterior jets issuing from the multiple

orifice manifold would provide the necessary energy dissipation. There were, however, serious questions as to just how the energy dissipation would dispose itself along the by-pass flow route. Surging and instability in the vertical pipe with high turbulence and flow asymmetry in the manifold jet region were anticipated. These actions could conceivably produce surges and waves in the cooling tower basin and excessive local structural loadings appeared possible. A hydraulic model study was considered necessary to establish the disposition, nature, and magnitude of flow abnormalities resulting from the energy dissipation and to determine corrective measures if needed. Model tests equivalent to the primary flow rate of 126,000 gpm and to the short term emergency flow rate of 168,000 gpm were specified.

III. The Cooling Basin Sump - Its Function and Problems

The proposed arrangement of the cooling towers and main pump house as shown in Fig. 1 involves a simple connecting piping layout but one which imposes an asymmetrical flow pattern in the withdrawal at the downstream end of the cooling tower basin. The withdrawal sump consists of a simple sharp-edged rectangular depression or sump in the basin floor. This sump is fitted with a 144 inch diameter discharge pipe as shown in Fig. 6. Although there was no concern with possible major flow disturbances, vortex formation with local high velocities and air entrainment was a remote possibility with this asymmetrical arrangement. Inclusion of a hydraulic model study of this system component was considered desirable to evaluate these possibilities. Model tests equivalent to flow rates of 126,000 and 168,000 gpm were specified.

IV. The Pump Basin - Its Function and Problems

The pump basin as shown in Figs. 1, 7, and 8 serves to provide a flexible free-surface interconnection for flow between the two cooling towers and the two recirculating pumps. In operation, the basin could receive water from either one or both of the 144 inch tower discharge pipes which feed into the north end of the basin. Water could be drawn from the south end of the basin through either or both of two 120 inch suction bellmouths supplying the two circulating pumps. These 78 inch by 66 inch, double suction, centrifugal pumps are each powered by two-speed motors of 5,000 horsepower.

The basin, as shown in Figs. 7 and 8, contains one small central support pier and three large structural support piers which also mount fixed trash screens. Included in the arrangement is a small auxiliary sump on the west side. This provides water supply for auxiliary plant pumps and a fire protection pump which may draw 2,000 gpm. Also included, as shown in Figs. 9 and 10, are rectangular gates which may be used to close off the pump bellmouths to permit unwatering the pumps (in the model only the major outline of the open gate elements influencing flow have been included).

The trash screens which may plug in random patterns might significantly contribute to basin flow patterns which in turn could be detrimental to pump performance. The trash screens which are to be of No. 10 gage stainless wire in a 3/4 inch mesh would produce a negligible head loss in the clean condition and with the design velocity of about 1/4 ft/sec. It was, however, specified that the influence of the screens should be examined for a condition of 50 percent blockage.

By the nature of their simple plane-form, concrete construction, sumps with rectangular cross-sections necessarily impose abrupt area and shape changes on the cross-sections of the flow stream passing from an entering circular pipe to an exiting circular pump intake. These transitions inherently generate vorticity and turbulence. Large vortices when conveyed to the leading edge of the pump impeller blades introduce local abnormalities in the vector alignment of the flow with the blade. Such misalignments when persistent may cause serious flow separation and cavitation with consequent performance loss, loading transients, vibration, noise, mechanical damage or metal erosion. Vortices of sufficient size and strength to suck air into the pump from the basin water surface impose especially severe conditions at the pump.

Because of the complex and varied nature of the possible flow routings in the basin and the inherent vortex generating capabilities of all rectangular sumps, it was considered essential to evaluate the vortex potentials of the proposed basin design. To this end, model hydraulic flow tests were specified in accord with Fig. 12.

It was also specified that the pump manufacturer (in this case Allis-Chalmers) should examine the model of the proposed design and its modifications and confirm its compatibility with the pump to be supplied.

V. Pertinent Full Scale Design and Operating Conditions

The general layout of the cooling towers is largely determined by the prevailing wind patterns at the plant site and the location of the generating plant on the site. The recirculating pumps are located mutually convenient to these cooling towers and the heat source at the steam condensers in the generating plant. The pumps are located so as to process cooled water with a working range from 35 to 88°F. These considerations lead to the general layout shown in Fig. 1.

The discharge requirements of the pumps are established by the heat rejection requirements of the steam condensers and auxiliary cooling water heat exchangers. The head requirement for each pump is the summation of the friction head requirements of the condensers, the basins, auxiliary cooling water heat exchangers, and the connecting piping plus the vertical lift needed to supply the gravity distribution and drip-spray in the cooling tower. (The latter value is approximated by a 43 foot head between the crown of the distribution pipe and the free surface of the water in the tower basin.)

The foregoing head-discharge requirements lead to the preliminary selection of a double suction, single stage, centrifugal, two-speed pump with a rating of 167,000 gpm at 96 foot head when driven at 391 rpm by a nominal 5,000 hp motor and when operating in parallel. The alternate pump speed is 320 rpm. The pump has a 78 inch suction, 66 inch discharge and carries the designation of WSDD by its manufacturer, Allis-Chalmers. The performance characteristics for the selected pump are shown in Fig. 11.

A variety of combinations of pumps, speed and flow routings are conceivable in normal and emergency plant operations with possible varying influence on vorticity generation in the pump basin. In consequence, it was specified that the conditions of the table of Fig. 12 should be examined in the hydraulic model to establish potential flow difficulties and the solution to such difficulties.

Stage levels for the water fill in the system are taken as El. 972 for no-flow conditions with the pump basin dropping to El. 971 as flooding of the tower distribution system takes place under pump action.

The 60 inch butterfly valves in the header distributor and the 84 inch by-pass butterfly are remotely controlled from the control center during plant operations. The valves are intended to operate either open or closed. Transient surges in the pump basin and the pump discharge lines were not considered to be a problem in full-scale start-up operations. It was assumed that the very large free surfaces of the cooling tower and pump basins together with proper pump start-up procedures would provide sufficient damping to prevent surging or resonance conditions. In consequence, the simplified open circuit gravity supply and discharge system as shown in Fig. 13 was considered adequate for the model study.

The debris screens located in the pump basin were presumed to encounter only modest loading over a long time span. In consequence they are not to be mechanically cleaned in place but rather will be replaced by a cleaned screen if and when needed.

The maintenance of a preferred chemical quality in the cooling water will from time-to-time require the injection of adjusting chemicals into the water. It is proposed to house the necessary equipment and stored chemicals in the pump house and inject the chemicals into the pump basin water at the point shown in Fig. 7. It is important that the strong chemicals be quickly and effectively diluted in the receiving water with only low concentration coming in contact with system materials. Injected dye patterns were to be studied in the hydraulic model to evaluate the dispersion characteristics of the proposed system.

VI. The Hydraulic Model

A. General Considerations

The objective of the hydraulic model study of the cooling system was to provide a set-up in which flow processes would reasonably simulate comparable conditions in the full scale installation. The model was to permit operational programming of all specified flow variables which might be pertinent to system performance and was to permit observation and evaluation of these flow effects at reasonable cost.

In this instance the model was fitted to an existing Laboratory water supply and space constraints. These constraints lead to the Laboratory disposition of the model and its three focal study areas as shown in Fig. 13.

This resulted in an undistorted model with a 1 to 12 ratio of model length to full scale length. Experience has shown that this type of model and scale ratio are relatively free of obscuring scale effects. It should be noted that space constraints dictated that in the model the alignment of the pipe connecting the cooling tower and the pump was changed from that shown in Fig. 1 with an elbow and dog-leg being added in the model.

A model with free surfaces in the focal test areas is generally considered to have its basic flow patterns primarily generated by the gravity force. The model occurrences will then have a relation to the full-scale in accord with the Froude law. This requires that all length values be in accord with the length ratio $L_m/L_{fs} = 1/12$, all velocity and time values in accord with $V_m/V_{fs} = [L_m/L_{fs}]^{1/2}$ or $= 1/3.46$, and all discharge values in accord with $Q_m/Q_{fs} = [L_m/L_{fs}]^{5/2} = 1/500$.

Many experimentalists when working with models associated with hydraulic machinery run tests at Froude velocities and in addition run check tests at either full scale velocities or the highest velocity practically attainable in the model. Such tests aid in determining whether physical forces other than gravity are significant in the establishment of flow patterns. Limited check tests of this type were provided for in the modelled pump basin but were not considered necessary nor practical for the recirculating by-pass and cooling tower modelling.

In the layout shown in Fig. 13 water was supplied to the model by gravity flow from the Mississippi River via 12 inch and 6 inch pipes under a head of about 45 feet. Flow control valves with adjacent calibrated orifice meters permitted readily establishing desired test inflows in the model. Outflow from the pump basin is by gravity, using 6 inch pipe lines discharging into a sub-floor waste trench. Stage level in the basins and the rate of outflow was established by control valves in the discharge lines. The discharge lines are shown in Fig. 14.

B. The Recirculating By-Pass

The full-scale by-pass system shown in Fig. 2 was modelled in transparent acrylic beginning at the upstream end of the distribution header at the top of the tower as shown in Fig. 4 . The two 60 inch distribution lines

were dummied up to the position of their butterfly control valves where the lines were blanked off. The 84 inch butterfly valve, which controls header flow into the by-pass, was modelled only by a distributed cylindrical approximation of the blockage area existent within the pipe when the valve was open. The valve simulated was a Triton-XL type manufactured by the Henry Pratt Company.

The elbows and drop pipe were modelled in acrylic and a piezometer well, with a stage scale reading damped pressure values, was attached to the horizontal pipe following the lower elbow. A second pressure tap and piezometer well were provided at the downstream end of the manifold pipe. The two piezometers permitted reading a rough approximation of the hydraulic gradient existing within the manifold pipe.

In the original design of the perforated manifold, as shown in Fig. 4, the pipe was made of transparent acrylic with a hole pattern as shown in Fig. 16(a). In a later version, as shown in Fig. 5, the pipe was modelled in metal because of difficulty in machining the close-spaced holes in an acrylic pipe. The hole pattern in the revised version is shown in Fig. 16 (b) and (c).

Two transparent air vent stacks were added to the revised version of the manifold to clarify the air release action and to show the relative stability of undamped pressure values along the perforated pipe. The position of the stacks are shown in Fig. 16(b) and in the right background of Fig. 5.

In the revised version of the model manifold, turning or flow straightening vanes were added to the exterior of the manifold pipe as shown in Fig. 5 and as detailed in Fig. 17.

The cooling tower basin, including the floor depression, upstream piers and floor ramps associated with the recirculating by-pass system, were modelled as shown in Figs. 4 and 5. In a later version a sealed enclosure slab was added above the free surface of the manifold chamber as shown in Figs. 5 and 16(b). This slab was modelled in clear acrylic. PVC plastic sticks were used to model the 4 x 4 inch wood posts used to support the lattice works of the full-scale tower.

In a revised arrangement the continuous L beam shown in Fig. 3 was raised from an original base elevation of 971 to an elevation of 972.

The sidewalls of the modelled manifold chamber and cooling tower basin were fitted with colored marking tapes spaced to show surface stage values equivalent to one foot of stage in full scale.

C. The Cooling Basin Sump

The cooling basin and downstream sump was largely modelled in wood. The general arrangement is shown in Fig. 15.

D. The Pump Basin

The pump basin and structural support piers were largely modelled in wood and fitted with marking tapes spaced to show surface stage values equivalent to one foot of stage in full scale.

In the full-scale basin screens are to be fitted across the four bays formed by the basin walls and the three large structural piers shown in Fig. 8. These screens are intended to serve as a barrier to debris or solids which might impair the action of the pump or condensers. Because of the coarse character of the screens and the very large area of the basin section where they are located, in normal operations the clean screens would produce no significant head loss. In consequence, they would have no significant effect on flow patterns generated in the basin and, thus, they were not modelled. However, if significant debris did occur in operation and if this debris were not removed, the partially plugged screens could have a significant effect on basin flow patterns. This effect would be most significant if the position of certain plugged screens happened to produce strong asymmetries in the general flow. In order to test these influences, the four screens located in the model were provided with removable full length screens. These screens were arbitrarily made of a thin perforated steel sheet in which 1/4 inch holes were staggered on 5/16 inch centers (3 inch holes on 3-3/4 inch centers in full scale). This plate had 58 percent of its area open and simulated a partially plugged screen. Figure 8 shows one of these four screens installed in place.

The model pump basin included the small separate basin on the west side of the main basin. This west basin draws water from the main basin to supply

the plant fire fighting system with 2000 gpm of flow via a vertical pump located as shown in Fig. 7. In the model the fire pump was simulated by a 1-1/2 inch pipe with its lower end positioned 3/4 inch above the floor and controlled to pump 4 gpm. No attempt was made to model withdrawal of water by the auxiliary plant service pumps because these pumps do not operate when the large cooling pumps operate.

The model pump basin also includes a simulation of the vertical sluice gate which will be used to achieve closure of the entrance to the suction pipe leading to the pump. This gate is to be closed only infrequently when unwatering of the pump is required. It is normally open. In the model only the bulk features of the wide open full-scale gate were included. The gates were modelled after the 120 inch by 120 inch Series #HY-Q-120 as made by the Rodney Hunt Company and shown in Fig. 9. The resulting model assembly is shown in Fig 10.

Model evaluation of the flow quality entering the suction side of the double-suction circulating pumps did not necessitate the presence of working pumps. Flow was, instead, generated by suction withdrawal of water through a gravity pipe discharge system. For evaluation and observation, short cylindrical lengths of transparent test section were installed in each of the basin discharge lines just downstream of the flanged exit of the contracting bellmouths as shown in Fig. 14.

One of these test sections was fitted with a Pitot cylinder mounted on a diameter of the test section. The test section could be rotated to permit positioning the Pitot probe on either a horizontal or a vertical diameter. The Pitot could be stroked or traversed along the diameter to permit successive point determinations of velocity values from wall to wall of the cylindrical section thus leading to a full plot of the velocity distribution. The physical arrangement of the contracting bellmouth, the cylindrical test section, and the velocity traversing Pitot are shown in Fig. 14.

As shown in Fig. 18, one of the 1/4 inch Pitot insertion holes in the transparent window section was alternately connected to a vertical 1/8 inch inside diameter piezometer. This gage glass was relatively undamped and was used as an approximate measure of wall pressure fluctuations in the plane of the pump suction.

The second of the two cylindrical test sections was fitted with an array of five independent vortex sensors mounted along an upstream diameter of the test section. Each sensor was a bladed rotor with a flat blade having all blade chords and the rotor axis positioned parallel to the test section axis. Such sensor blades will evidence no rotation when placed in a purely axial flow but will spin rapidly when exposed to local vortices with axis parallel to that of the test section. The array of five rotors (each equivalent to one foot diameter in full scale) across the 6 foot 6 inch full-scale diameter of the suction pipe permitted complete sensing of harmful flow vortices along the selected diameter. With the rotor array mounted on a rotatable shaft located on the test section axis and controlled from the pipe exterior, the five sensors could be slowly swept around to probe the entire circular section for the presence of vorticity. Fig. 19 shows the vortex sensor assembly which is mounted inside the test section while Fig. 14 shows the external stem used to rotate the assembly and the external positioning protractors.

Additional information on the quality of flow entering the pumps can be obtained from visual or photographic records of the motion of small flags or streamers positioned on the entrance edge of the suction opening in the basin wall. For these tests short lengths (about one foot full scale) of yarn were attached to the entrance lip. If the quality of the approach flow is good, there will be little or no rotational components in the streaming direction of the yarn. If the flow is steady and devoid of large scale turbulence, the streamers will be essentially steady in position. If turbulence is present, the nature of the flutter sweep of the streamers will indicate the relative size and frequency of flow disturbances. Fig. 10 shows the configuration of the entrance and the clock-hour position of the 12 streamers arranged around the entrance. The angular elements of the frame of the unwatering gates as shown in this figure can contribute significantly to local flow disturbances which may be evidenced by the flow streamers.

VII. The Model Observations

A. The Recirculating By-Pass

a. Flow in the Distribution Header and Vertical By-Pass Pipe

For all specified operating conditions and for both of the manifold hole perforation patterns shown in Fig. 16, the flow exitting from the freely vented header through the open 84 inch control valve produced a free-fall condition at the header outfall. This is confirmed by the observations in Fig. 20.

In such an outfall the flow passes from a sub-critical flow in the header to a super-critical flow in the vertical downcomer. In consequence, the header flow is oblivious to the various flow conditions that may exist in the lower portion of the by-pass, provided free venting is maintained in the upper portion of the falling jet and provided backwater effects do not submerge the overfall from below. Since, as shown in Fig. 20, neither of the latter conditions prevailed, the header flow found and maintained a stable pattern when steady flow conditions were achieved.

Some question existed regarding the nature of free surface transients or surges which might occur during pump start up. Surges of this kind can occur in some piping configurations with resulting impact pressure values of destructive magnitude. The estimated time-discharge curve for the proposed pumping system was provided by Black and Veatch and is as shown in Fig. 21. In this curve the bulk of the full-scale change in discharge rate is achieved in about 20 seconds with a trail-off to 60 seconds for full discharge. A manual butterfly valve was installed in the gravity supply line for the model flow with a stop provided for a full steady flow equivalent to $Q = 168{,}000$. It was assumed that a simple manual valve opening action in a span of 8 to 10 seconds would provide a model flow roughly approximating the full-scale condition. This is based on a model to full-scale time relation of 1:3.46 as discussed in Section VI.

Model operations under the above conditions gave no evidence of surge or impact loadings in the header, but only a gradual upwelling, filling, and overflow. There appeared to be no need for additional start-up controls.

b. Flow in the Lower Elbow and Manifold Interior

The interior flow in the elbow and manifold model, with the original hole arrangement as shown in Fig. 16(a), is shown in Fig. 22. The general pattern of flow was much the same for both the large and small flow conditions. In this pattern the bulk of the flow jetted down the west wall of the vertical downcomer in a free fall accelerating action and passed around the outside of the elbow and well into the manifold in a discrete flow stream. The depth of this flow stream increased with the discharge. The velocity of the stream exitting from the elbow was estimated to be about 55 fps. The flow energy in this stream was estimated to be 1800 HP for the large flow and about half this for the small flow. It was assumed that little energy was lost in the free fall process.

The throttling resistance of the manifold orifice holes provided pipe filling or a back-water within the manifold pipe. This back-water interacted with the high velocity jet entering from the elbow to produce a hydraulic jump type of flow expansion with a slowly circulating roller submerging the elbow jet. The roller extended back to the elbow exit. The large scale turbulence generated in the jump and roller decayed to a smaller scale as the flow proceeded through the manifold pipe. However, violent axial surging occurred along the entire length of the lower pipe.

Large amounts of air were entrained into the flow in the roller and jump mechanism and the bulk of this air was expelled from the manifold pipes with the jets issuing from the upstream half of the jet holes.

A pressure tap and gage glass located on the pipe sidewall a short distance downstream of the elbow indicated that the pressure within the jump roller was essentially atmospheric. The presence of an atmospheric pressure indicates that the jet discharging from the top elbow did not serve to seal the downcomer from atmospheric intrusion. This was confirmed

when the normally vented upper end of the downcomer pipe was alternately covered and sealed. Under sealed conditions, a significant vacuum soon developed. Full venting was employed in all subsequent tests.

A pressure tap and gage glass located at the downstream end of the manifold pipe showed a damped average pressure head equivalent in full scale to about 13 feet above the pipe centerline or El. 979.5, for the maximum discharge of 168,000 gpm. Other studies at the Laboratory dealing with pressure transients in hydraulic jumps suggest that wall pressure fluctuations of $\pm$ 20 feet of head might be expected as transient hydraulic loads on the pipe walls.

In the revised version of the manifold, as shown in Fig. 5, Figs. 16(b) and 16(c), and Fig. 17, tests similar to those previously described were carried out. In these tests the most significant changes were:

1. The additional resistance provided by the smaller size and number of manifold holes caused the hydraulic jump to move further upstream with major jet expansion occurring within the elbow rather than downstream in the manifold pipe. This is shown in the photos of Fig. 23. As a consequence of this, the pressure head just below the elbow increased substantially to a level of about El. 974.0 for Q = 126,000 gpm and El. 979.0 for Q = 168,000 gpm. Corresponding pressure heads at the downstream end of the manifold pipe were El. 981.0 and El. 985.0.

2. The foregoing increase in elbow pressure significantly reduced the slope of the pressure gradient along the manifold holes. This tended to improve the uniformity of velocity distribution across the tower basin.

3. The flow in the pipe as it enters the manifold shows large air bubbles and air slugs surging back and forth violently near the top of the manifold with a high level of turbulence.

4. The two vent stacks located at the top of the manifold were topped out in the model at El. 988 or 21.5 feet above the

centerline of the pipe. Despite the height of the stacks, slugs of foam were frequently projected from the top of the upstream stack and large slugs of water were intermittently projected from the downstream stack as shown in Figs. 24(a) and 25(a).

5. Tests with the stacks removed and stack holes plugged produced no evident change in Items 1 to 3 above so subsequent tests were made with stacks removed.

c. Flow at the Manifold Exterior and Basin Entrance

The dispersed pattern of jet holes in the manifold shown in Fig. 16 serves as a second stage energy dissipator and flow distributor in the recirculating by-pass system. With internal manifold pressures being considerably above the exterior pressure, jet discharge occurs through the holes and an external pattern of flow peculiar to the jet pattern will develop. Discharge of these high velocity jets into the relatively quiescent water of the cooling tower basin produces a rapid jet expansion with entrainment of the surrounding basin water and a decay of the jet velocity. This action results in a local high level of turbulence with dissipation of the jet energy. Because the flow velocity and pressure in the interior of a manifold pipe varies with axial movement along the pipe, manifold flows tend to produce an unbalanced distribution of flow in the receiving basin. In consequence, the distribution of holes in a manifold frequently requires experimental adjustment to achieve desired flow patterns.

The following observations were made for flow conditions resulting from use of the original pattern of holes as shown in Fig. 16(a).

1. Near the upstream end and bottom of the manifold pipe high internal axial velocities occur. In consequence, upstream jets angle strongly from west to east as they jet from the manifold into the basin.

2. The gradient of pressure along the manifold axis provides highest pressures near the downstream end. In consequence, holes near the downstream end pass greater discharge than those near the upstream end. With the near-uniform distribution of holes shown in Fig. 16(a), a non-uniform distribution of flow occurs at the entrance to the receiving basin.

3. With the manifold holes located below the pipe center, the discharging flow is stronger near the bottom and a return flow is required near the water surface to provide flow for entrainment into the expanding jets. This strong return was most evident along the upstream one half of the manifold.

4. As mentioned in Item(b) above, a large amount of air was contained in the flow within the manifold and this air was discharged with the manifold jets. Most of the air was contained in the jets discharging from the upstream one half of the manifold length. Most of the air bubbled to the water surface in the manifold basin upstream of the continuous L beam shown in Fig. 3.

5. A significant boiling or agitation of the water surface in the basin occurred beginning near the middle of the basin and prevailing to the east wall of the basin. The upheaval was largely contained below a surface elevation of 973 and no crawl-up on the side wall occurred above this level. The structural continuous L beam took some flow buffeting on the upstream side and on its bottom.

6. It was estimated that the recirculating by-pass at Q = 168,000 gpm dissipated about 80 percent of the initial potential energy of the header flow within the elbow-manifold leg and about 20 percent in the jet discharge into the basin. For the minimum flow of Q = 79,000 gpm only about 3 percent of the energy was dissipated in the manifold jets and flow into the basin was relatively calm.

7. Although the flow in the cooling tower basin near the west wall was confused and the velocity was not uniformly distributed across the basin width, the flow was contained within the basin and surface waves were well below the freeboard provided by the design.

In the revised version of the manifold, as shown in Figs. 5, 16(b), 16(c), and 17, tests similar to those described above and other tests were carried out. In these tests the most significant changes were:

1. The presence of the turning vanes on the exterior of the manifold pipe greatly reduced the strong lateral jet action previously evidenced.

2. The greater manifold pressures, as discussed in Item 1 relating to the manifold flow, produced higher velocity exterior jets than previously. This produced a strong aspirating action in the lower portion of the chamber upstream of the cross beam. This evidenced itself as a strong upstream flow at the surface.

3. The use of a new ceiling or roof over the manifold chamber of a tight or sealed construction caused an air dome to collect below the roof. The source of the air is in the jets discharging from the manifold. The flow action at the base of the vertical downcomer pipe of the by-pass entrains a large amount of air into the flow entering the manifold pipe and much of this finds exit through the orifice jets. Much of the jetted air gravitates upward and is collected under the roof dome although a considerable amount is carried out directly into the cooling tower basin where it surfaces as shown in Figs. 24(a) and 25(a). The domed air progressively builds up and depresses the level of the water in the manifold chamber until the air finds release by bubbling out under the cross beam at the upstream end of the cooling tower basin. This action is quite harmless but does impose a gas pressure head equivalent to about one foot of water head on the underside of the roof. (This presumes that the stage level in the cooling basin is at El. 972 and the bottom of the cross beam is at El. 971.)

4. Venting of the accumulated gas dome by three holes, equivalent to 9 inch diameter full-scale, released most of the pressure and the water level in the manifold chamber rose one foot. Subsequently, the cross beam was raised one foot (to El. 972) and with vent holes closed, the water level inside and outside the manifold chamber settled to El. 972.

5. Figures 24(b), 25(b), and 26(b) were taken with a brief time exposure with paper confetti scattered on the water. The dark line underwater is the end of the floor ramp between the manifold chamber and the tower basin. The cross beam is with its base at El. 971 and a captured air dome exists over the water surface in the manifold chamber. Flow is from top to bottom. The small disk at the right in the photos was rotating at one revolution per second and had a single white radial line on a black background. The pie-shaped gray area on the disk is the sweep of the radial line during the camera exposure. The sweep width in these photos shows an exposure time of about 1/8 second model or 0.125 x 3.46 = 0.432 seconds of time in the full-scale event. This time, together with knowledge that the spacing of the support posts is 4 foot by 8 foot full-scale, provides a rough measure on the confetti streak lengths or the velocity of the surface water.

6. It is evident from Figs. 24 - 26 that considerable flow confusion exists at the water surface above the floor ramp where some upstream flow must be maintained to feed the entraining action going on with the lower level jets. The surface flow becomes more orderly as flow proceeds downstream.

d. Flow at the Upstream End of the Cooling Tower Basin

The surface flow at the upstream end of the tower basin as shown in Figs. 24 - 26 indicated some confusion of pattern and mal-distribution of velocity across the basin. To further clairfy the nature of the flow below the surface, velocity values were measured at selected points in the cross section with a small Ott current meter.

The current meter with a rotor of 1-1/4 inch diameter (diam. = 15 inches full scale) was axially positioned with rotor tips about 1 inch (12 inch full scale) above the basin floor in a selected station and again 1 inch (12 inch full scale) below the water surface for an alternate run at the same station. The average of these two velocity runs was considered the velocity at the station.

The selected stations for the traverse were located at a section of the cooling tower basin which is 15 inches (15 feet full scale) downstream of the end of the floor ramps rising from the manifold chamber. This is approximately at the center of the timing dial shown at the right in the photos of Figs. 24(b), 25(b), and 26(b). Because of the local flow disturbance created by the presence of the support posts, the selected stations for measurement were located midway between the posts which are positioned as shown in Fig. 3.

The measured velocity values are plotted in Fig. 27 as simple bar diagrams for the test cases where all of the straightening vanes are attached to the manifold and the alternate case where the vanes on the downstream half of the manifold have been removed. Velocities of less than 3/4 fps in the full-scale were below the operating threshold of the current meter employed for observations in the model. Flow regions with values less than this threshold are so indicated in Fig. 27. In these tests the cross beam was raised to a bottom El. 972 and no surcharge air pressure existed over the manifold chamber.

The velocity distribution plottings suggest the following:

1. The velocity distribution with all turning vanes installed is in general more uniform than the distribution with vanes installed only on the upstream one half of the manifold pipe.

2. When the downstream one half of the vanes are removed, a strong high velocity region occurs about 10 feet out from the ease wall of the basin.

3. Removal of the remainder of the vanes would undoubtedly promote a greater west to east cross-flow from the westerly or upstream orifices. This would further strengthen flow along the east side of the basin and weaken flow along the west side.

4. Of the limited cases tested, the case with all vanes installed appears to provide the best velocity distribution in the tower basin.

B. The Cooling Basin Sump

The general character of the flow pattern approaching and within the basin sump is delineated in the photos of Fig. 28. These photos show a generally axial basin flow which proceeds from the top to the bottom. Also shown for the approach

flow is a fairly uniform distribution of velocity across the basin as depicted by the length of the confetti streaks. The time exposure in the model photos is about 3/8 second (.375 x 3.46 = 1.29 seconds full-scale).

The general pattern of the basin approach flow is relatively stable with time but conditions in the extreme southeast corner of the sump change rapidly with time. The photos are thus only typical. The confused discharge flow in the sump corner involves a complex pattern of flow separations and vortices generated by three 90 degree changes in direction and a cross sectional shape change from rectangular to circular. While the flow character is complex, the generous sizing of the flow sections produces only modest velocities and weak vortex patterns. In consequence, vortex centers did not produce significant surface depression and general stability prevailed for the flow entering the 12 foot discharge pipe.

There was no evidence of a surface depression as the flow passed from the basin to the sump.

The sump performance appeared to be wholly acceptable.

C. The Pump Basin

a. Surface Vortex Observations

In accord with the operating conditions specified in Fig. 12, the pump basin model was observed to detect any evidences of major organized flow vortices generated in the basin and fed into the pump intakes. Initial observations of vortex structure looked for surface vortices above the pump intakes. Particularly sought were vortices with considerable strength sufficient to depress the surface and suck air down into the pump intake.

Under all specified operational flow conditions and including extra tests in which the basin surface level was lowered as much as 12 feet full-scale, no stable air sucking surface vortices were observed. It appeared that expansion of the pipe jets on entering the basin produced a considerable level of turbulence which swept throughout the basin. The resulting turbulence remained random and constantly changing in pattern thus countering any tendency to develop stable vortices which could grow in strength.

Flow with two pipes feeding into the basin and two pumps drawing from the basin are shown in typical surface patterns in Fig. 29A. For this symmetrical condition strong upwelling of surplus entrained water occurs above the pump intakes and all incipient surface vortices are swept away from the intake.

For the case of one pipe supplying the basin and one aligned pump drawing from the basin, the surface flow as shown in Fig. 29B(a) shows a large general circulation with no strong vortices near the pump intake. When trash screens with 42 percent area blockage are installed on the principal flow route, the large general circulation is interrupted but again no strong vortices occur near the pump intake.

For the case of one pump supplying the basin and one non-aligned pump drawing from the basin, a generally poor flow routing is established. However, as shown in Fig. 29C, strong vorticity at the pump intake is not evident for either the flow without or with a resisting trash screen on the flow route.

All of the photos of Figures 29 were taken with high flow discharges. Flows with discharges diminishing to Q = 79,000 gpm evidenced a general weakening of vortex patterns. Flows using a super discharge of Q = 415,000 gpm showed a general strengthening of the turbulence pattern in the basin but no tendency to worsen vorticity at the pump intake.

Surface flow patterns were not significantly altered by adding a flow of Q = 2,000 gpm from the fire pump mounted in the small attached western sump.

b. Streamer Observations at the Basin Intakes for the Pumps

The flow indicating streamers described herein are located at clock-hour positions around the periphery of the bellmouth of the pump intakes as shown in Fig. 10. Flow character is evaluated in terms of the observed values of: (1) alignment of the flow with an axis generally parallel to the intake axis, (2) rapidity of oscillatory sweep about a mean axis of alignment, (3) angular range of oscillatory sweep about a mean axis of alignment, and (4) tendency to raise up from the bellmouth surface. The latter evidence occurs in dead-water regions of flow separation.

In general, for all flow rates and pumping arrangements the flow streamers were axial in direction for the mean of their sweep and remained close to the intake boundary surface. In the vicinity of the 3, 6, and 9 o'clock positions the streamer tended to raise from the surface. In such cases the uplift would sometimes raise to 90° from the surface and occasionally even reversed to indicate upstream flow. This condition at 3 and 9 o'clock was believed due to relatively weaker approach flows in these positions and to the close proximity of the streamer to the flow obstruction provided by the track

members of the unwatering gate. The abnormality for the 6 o'clock position was due to the proximity to the basin floor and the obstructing presence of the lower seat member of the unwatering gate. A somewhat weaker evidence of uplift and deviation from axial alignment occasionally was in evidence at the 2, 4, 8, and 10 o'clock positions.

The angle of oscillatory sweep back and forth about the axial alignment was generally less than 45°, but occasionally reached values up to 90° for the 3 or the 9 o'clock positions.

The rapidity of oscillatory sweep was generally moderate and fell off to a weak motion as the discharge value diminished.

In view of the fact that the flow cross-sectional area in the plane of the intake contracts in approaching the plane of the pump suction further downstream (the area reduces to 42 percent of the intake area), a strong stabilizing condition is exerted on the flow. In consequence, the relatively weak disturbances evidenced by the streamers at the intake will be quite insignificant as pump flow disturbances when they enter the pump suction.

c. Vortex Observations at the Pump Suction

The flow streamer observations just described were useful in evaluating flow misalignments existing around the periphery of the pump suction but were inadequate in describing flow character away from the periphery. In consequence, additional observations were made by probing the entire interior of the cross-section of the pump suction with small vortex sensors as described on page 11. This was accomplished by traversing the rotatable, multiple sensor shown in Fig. 19 around the plane of the suction opening. At points where the flow had no rotational components, the sensitive rotors gave no indication of rotation. Where the flow possessed weak and varying vorticity, the sensor blade would move back and forth slightly at a slow rate. Where the flow possessed a stable vortex structure, the blade would rotate steadily with a rate dependent on the strength of the vorticity.

For a variety of flow conditions, including a super discharge of Q = 415,000 gpm (full-scale), in the sump the observations of vorticity in the pump suction may be summarized thus:

1. Vorticity in most of the cross-section was non-existent or very weak and it was random in position and intermittent with time.

2. There were a few rare cases where a very slight but persistent rotation did occur.

3. There was no evidence of a strong, persistent vortex organization.

4. The randomness of the weak vortices is consistent with the observed continually changing pattern of eddies on the basin surface.

5. The continuing slight disturbances evidenced by the flow streamers at the 3 and 9 o'clock positions at the pump intake were not evidenced on the rotors at the suction of the pump. It appears that general flow turbulence and the contraction effects in the intake wiped out the local disturbances from the intake.

Observed vorticity at the pump suction appeared to be too weak and disorganized to significantly impair pump performance or life.

d. Velocity Profiles at the Pump Suction

Major asymmetry of velocity distribution in the flow approaching the suction of a pump may produce asymmetry or time variations of fluid loadings on the impeller. This may result in a wide variety of undesirable loadings on parts of the machine. To preclude the possibility of such loadings, the flow into the suction flange of the pump was evaluated with respect to the velocity distribution for the operating conditions specified in Fig. 12. The velocity distribution was measured with the Pitot arrangement described on page 10 and in Fig. 14. The Pitot was located downstream of the pump suction flange position, a distance equivalent to 2 feet full-scale.

Typical data from 7 point traverses of the Pitot cylinder along the horizontal and vertical axis of the pump suction plane are shown in Fig. 30. In this composite plotting the velocity values have been made non-dimensional by plotting the local value of the velocity as a percentage of the centerline velocity.

It is apparent from these plottings that no significant asymmetry of velocity is present along either the vertical or horizontal axis of the section. The profiles were essentially flat for all observed conditions.

e. Piezometric Boundary Pressures at the Pump Suction

The presence of repeating major flow transients or surges in the flow entering the pump suction may be detrimental to the pump performance and life. Due to the nature of the vortex sensors and the Pitot velocity measuring instrument, flow transients may have been present without being evident. A limited check on such pressure surging was made by installing a transparent piezometer tube of about 1/8 inch inside diameter (1.5 inch full-scale) in the model at the top of the pump suction as shown in Fig. 18. This relatively undamped piezometer was capable of responding to the larger and more significant pressure surges with a rough relative visual measure of the amplitude and frequency.

Observation of the piezometer tube during a wide variety of flow conditions showed relatively slow changes with a maximum range of head of about 1/4 inch model scale (3 inch full-scale). These values were consistent with the slowly changing eddy patterns evident in the pump basin.

The transients were not considered as significant to the performance of a full-scale pump.

f. Influence of the Trash Screen

The large mesh and fine wire of the proposed trash screens together with the low basin velocities where the screens are stationed imposes virtually no headloss or flow modifications when the screens are clean. However, in view of possible headloss and flow modification with partially plugged screens, it was considered desirable to check on the influence of the latter operating condition. This was done in the model by installing perforated steel sheets in the plane of the screen as described on page 9 and as shown in Fig. 8.

Model tests established that the partially plugged screens had a very significant effect on the basin flow pattern. When all of the four partially plugged screens were installed, they served to reduce the size and strength of vorticity and turbulence in the approach flow and to unify the velocity profile. However, when only part of the partially plugged screens were installed, their flow resistance altered the basic flow pattern through the basin and generated different patterns of vorticity (see for example Fig. 29B).

Although the alteration of pattern of flow was substantial in some cases, these alterations did not worsen the pattern of flow at the pump suction.

g. Influence of Fire Pump

It was not anticipated that the withdrawal of 2,000 gpm in the extension unit to the east of the main pump basin would significantly influence flow patterns in the main pump basin. However, several of the more important flow conditions in the model of the main pump basin were examined with and without fire pump withdrawal. The evaluation was made by observing scattered paper confetti on the water surface and noting changes in surface pattern.

It was noted that minor changes in pattern in the small extension sump did occur with fire pump operation but the pattern in the main basin did not change in any detrimental way that could be ascribed to fire pump operation. Subtle differences are, however, difficult to appraise, as the pattern in the main pump basin now is in itself not considered a significant factor on the performance or life of the circulating pumps.

h. Observations on Acid Injection Patterns

Page 6 and Fig. 7 include a description of the need for injection, the injection location, and the injection rate at which water quality controlling acid is to be injected into the water of the main pump basin.

In the model, provision was made for injecting a visually observable dyed water rather than actual acid at the location specified in Fig. 7. Model injection was also by way of a small pipe jetting directly downward into the basin. This injection is probably somewhat more forceful than the eventual full scale set-up where some form of terminal diffuser pipe would be employed. No details were supplied for such a diffuser.

The injection rate which was specified as 75 gpm for the full-scale was reduced to 75/500 gpm for the model.

Preliminary tests indicated that mixing action in the pump basin was good and diffusion of the dye occurred relatively rapidly. However, with continuous dye injection, visual or photographic observations proved useless shortly after injection began. To achieve more useful photo records of the dye movement, the technique was changed to a dye injection which lasted only about 5 seconds in model time. Sequenced photos beginning at 6 seconds after start-up were then initiated to record the travel and eventual dispersion of the dye cloud resulting from the short term dye injection.

The photos of Figs. 31, 32, and 33 record selected photos from the sequences taken with three different basic operating conditions. Fig. 31 shows dye patterns when flow enters the basin through Pipe A and exits through Pump A. Fig. 32 shows dye patterns when flow enters through Pipes A and B and exits through Pumps A and B. Fig. 33 shows dye patterns when flow enters through Pump A and exits through Pump B.

In the single pipe and pump operations of Figs. 31 and 33 the dye initially moves directly downstream in the direction of pipe flow and then a portion of the dye returns upstream along the far side of the basin. In the two pipe, two pump condition of Fig. 32, the dye initially moves directly upstream and a portion of the dye then moves downstream along the far wall of the basin. In all cases the dye appears to progressively disperse, dilute, and clear with time. It appears that acid injection in the full-scale basin should entail good mixing and dilution in the basin without high local concentrations of acid in either the basin or pump intake.

i. Observations by Allis-Chalmers Personnel

The model tests of the pump basin were primarily undertaken to assure that the proposed design of sump provided a "satisfactory" flow into the suction side of the circulating pumps. "Satisfactory" in this case is presumed to mean a flow which will permit the pumps, in normal operations, to perform in accord with the designed performance curves in a manner yielding low maintenance and long life. The evaluation of "satisfactory" flow consisted of establishing: (1) that no strong, sustained, or organized secondary flows or vorticity existed in the inflow, (2) that no strong asymmetry or abnormalities of velocity profile existed at the inflow, and (3) that no appreciable surging existed at the inflow.

In a visit on January 19, 1978, the performance of the pump basin and the evaluation systems were demonstrated to E. J. Fohr, D. L. Rehrer, R. P. Kunzelman, and W. D. Remmel of Allis-Chalmers; to J. R. Belden, R. J. Hemeyer, and E. B. Shannon of Black and Veatch; and C. Sannes and P. D. Colgan of Northern States Power Company. No criticism or recommendations for modification or upgrading of the evaluation system or the demonstrated flow characteristics of the hydraulic model were offered by those present. In consequence, the model study was assumed as satisfactory and testing was terminated.

VIII. Conclusions and Recommendations

The proposed recirculating by-pass system shown in Figs. 2 and 3 when fitted with: (1) the manifold orifice hole arrangement of Fig. 16, (2) the flow straightening vanes of Fig. 17, (3) an enclosure roof above the manifold chamber per Fig. 16, and (4) the continuous L beam raised to a bottom elevation of 972 and when operated in accord with Fig. 12, provided an acceptable energy dissipating system both within the manifold and within the manifold chamber. Moreover, the velocity distribution, surface roughness, and stability of the resulting flow entering the head end of the cooling tower basin was considered acceptable.

The substantial transient pressure loadings on the interior and exterior of the manifold pipe and elbow, as a consequence of the turbulent hydraulic energy dissipating mechanism, suggests that a rugged design for the pipe and its anchorage should be employed.

Limited observations in the model employing a simple start-up procedure indicates that the vented, recirculating by-pass system will not be subject to abnormal hydraulic loads as a consequence of pump start-up or shutdown procedures.

The design of the asymmetrical cooling basin discharge sump shown in Fig. 6, when operated in accord with Fig. 12, appears to introduce no detrimental flow characteristics to the cooling system.

The design of the pump basin shown in Figs. 7 and 9, when operated in accord with Fig. 12, appears to provide satisfactory hydraulic inflow conditions to the proposed Allis-Chalmers flow circulating pumps.

Operation of the proposed 2000 gpm fire pump concurrent with the main circulating pumps did not significantly influence inflow to the circulating pumps.

Limited photographic records of the path of acid injected into the pump basin for water quality control, indicates that the acid will readily disperse under the influence of inherent basin flow turbulence. No local build-up is apparent within the basin and the bulk of the acid is carried into the pump intakes shortly after injection into the basin.

The trash screens in the pump basin have no appreciable influence on flow patterns in the basin when used in a clean condition. However, a modelled screen when uniformly closed off 42 percent in area, significantly changed the pattern of flow in the basin. The changes in pattern were not detrimental to the flow quality of the water entering the pumps.

IX. Acknowledgements

Figures 1-3, 6, 7, 16, and 21 are adaptations of drawings supplied by Black and Veatch Consulting Engineers.

Figure 11 is an adaptation of an Allis-Chalmers curve as supplied by Black and Veatch.

Figure 9 is a reproduction of a drawing supplied by the Rodney Hunt Company.

Liaison between the St. Anthony Falls Hydraulic Laboratory and the Northern States Power Company was provided by P. D. Colgan of Northern States Power and liaison between the Laboratory and Black and Veatch Consulting Engineers was provided by G. Y. Gunn, F. E. Rickman, and J. M. Horner of Black and Veatch.

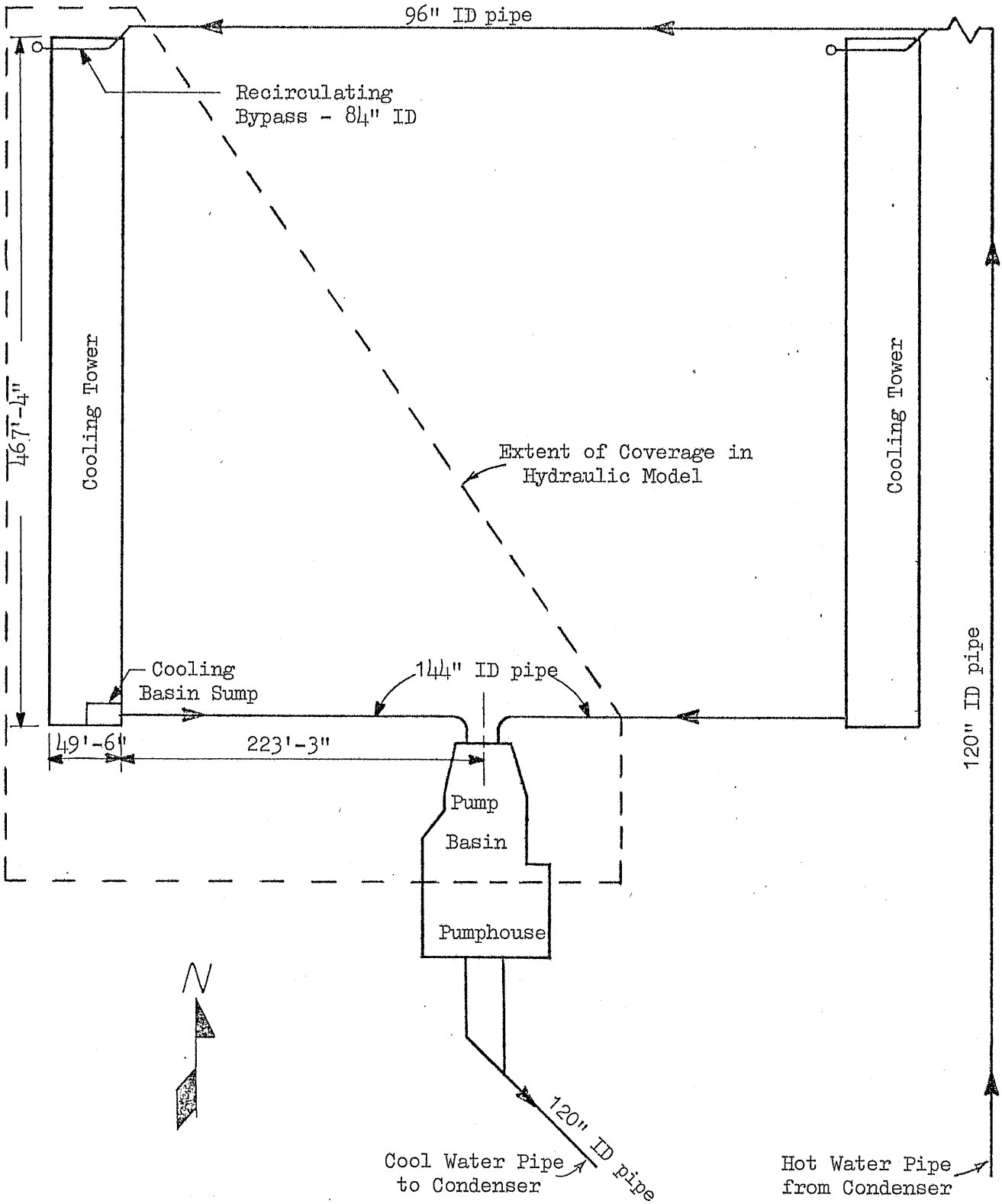

Fig. 1 - General Plan Layout of One of the Two Cooling Water Systems.

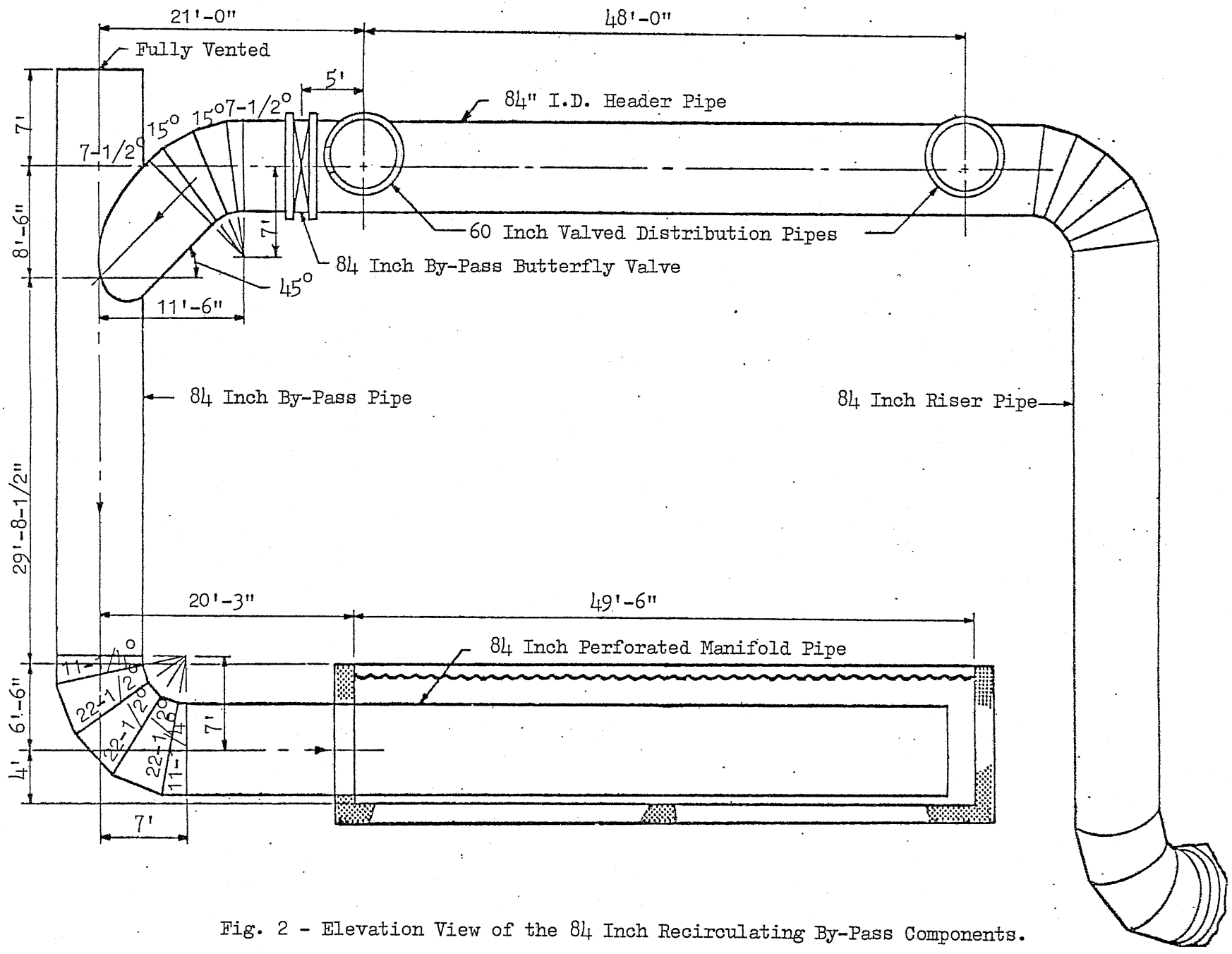

Fig. 2 - Elevation View of the 84 Inch Recirculating By-Pass Components.

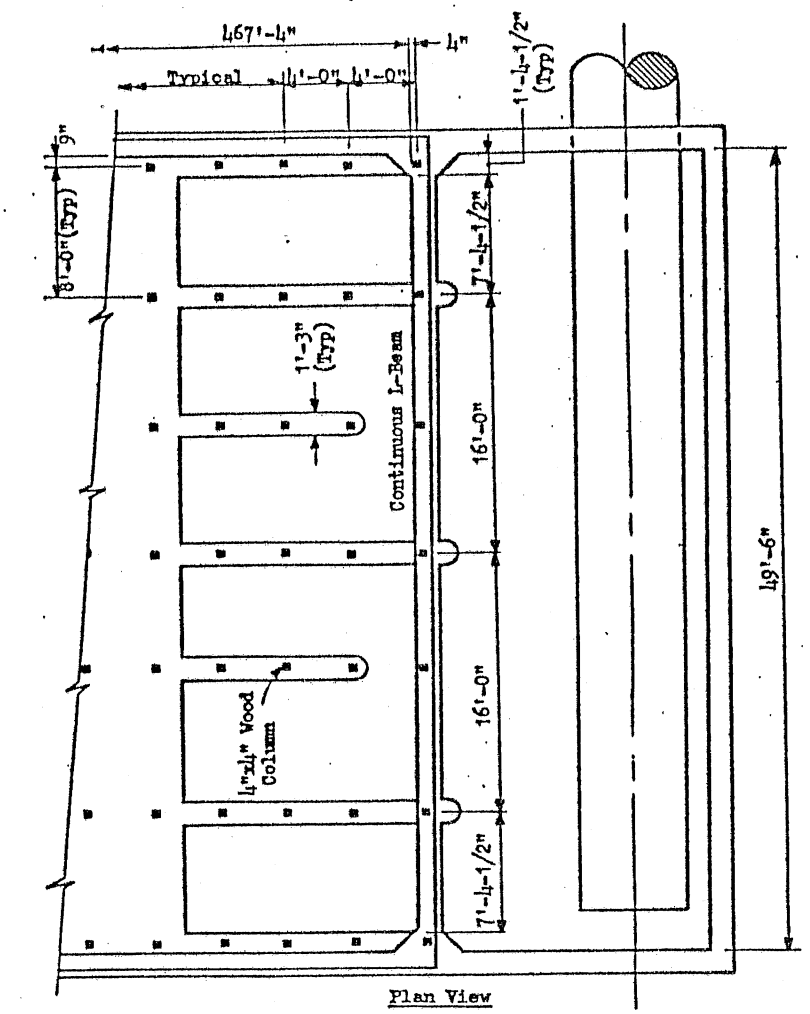

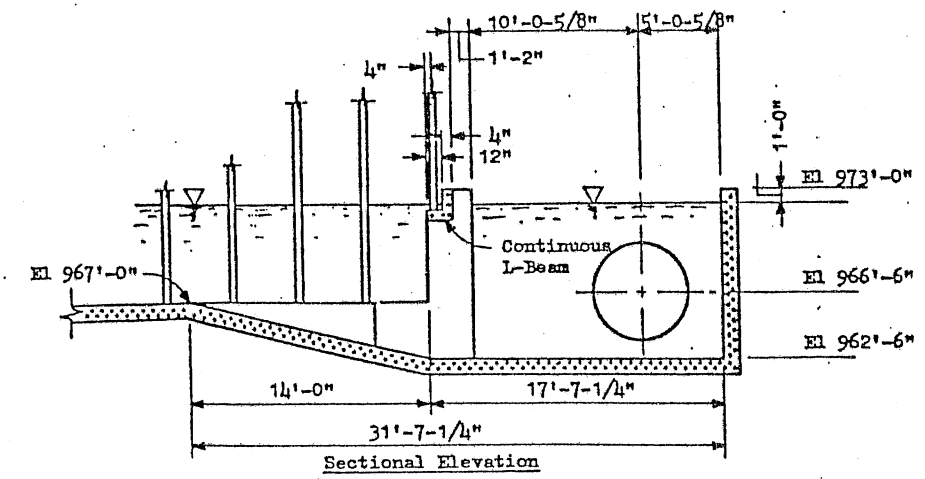

Fig. 3 - Plan and Section Details of the Manifold Chamber and Head End of the Cooling Tower Basin.

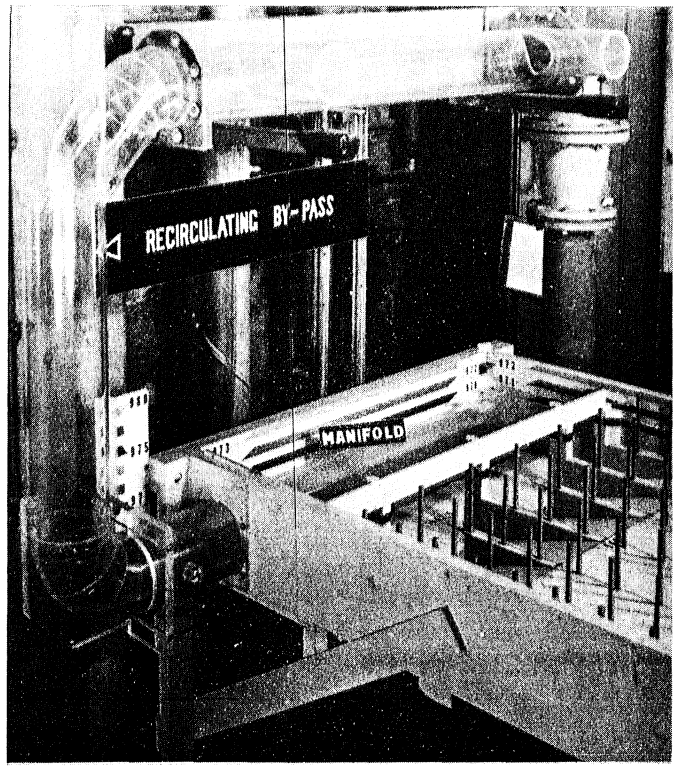

Fig. 4 - The 1:12 Model of the Recirculating By-Pass.

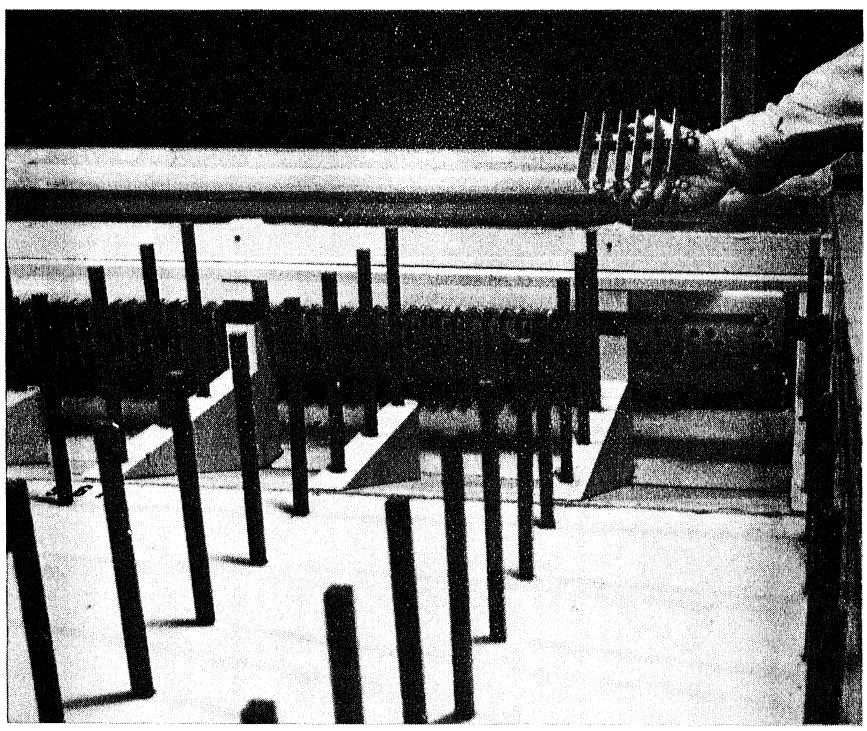

Fig. 5 - The 1:12 Modelled By-Pass Manifold Pipe and Manifold Chamber (showing revised manifold ports and exterior flow straightening vanes).

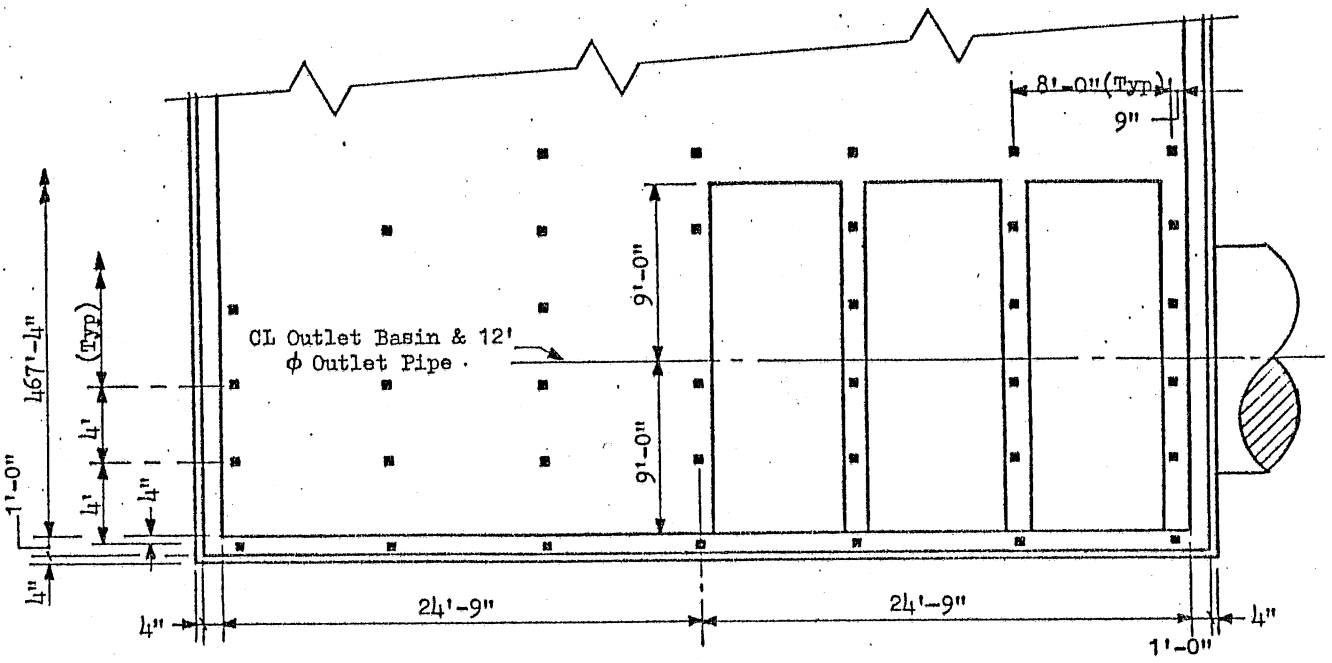

Plan View

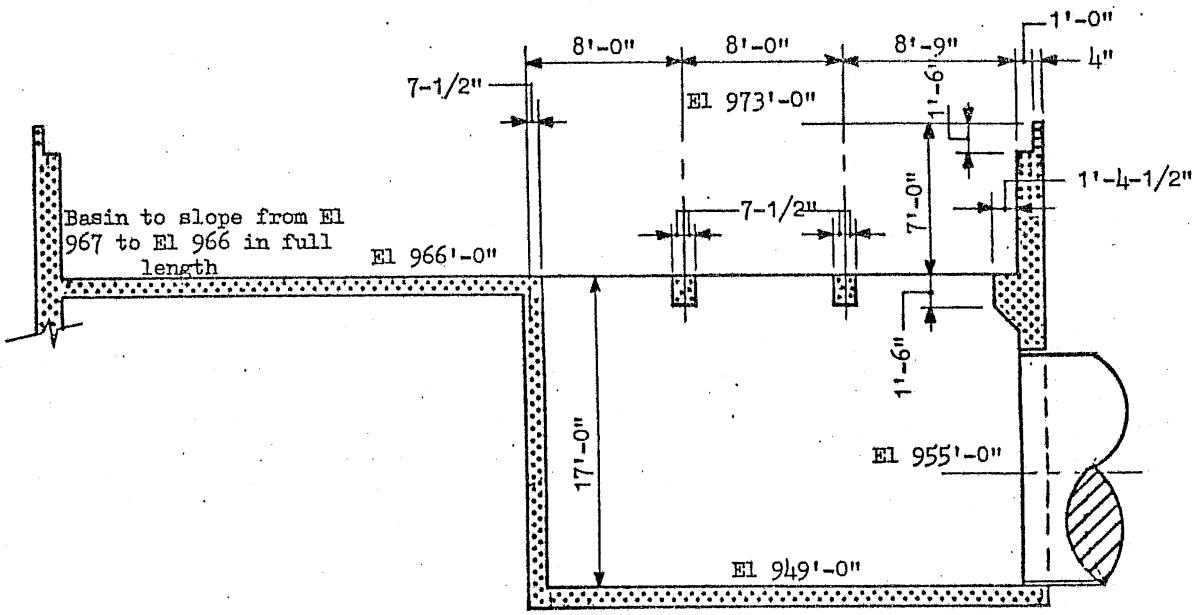

Sectional Elevation

Fig. 6 - Cooling Tower Basin - Sump Detail.

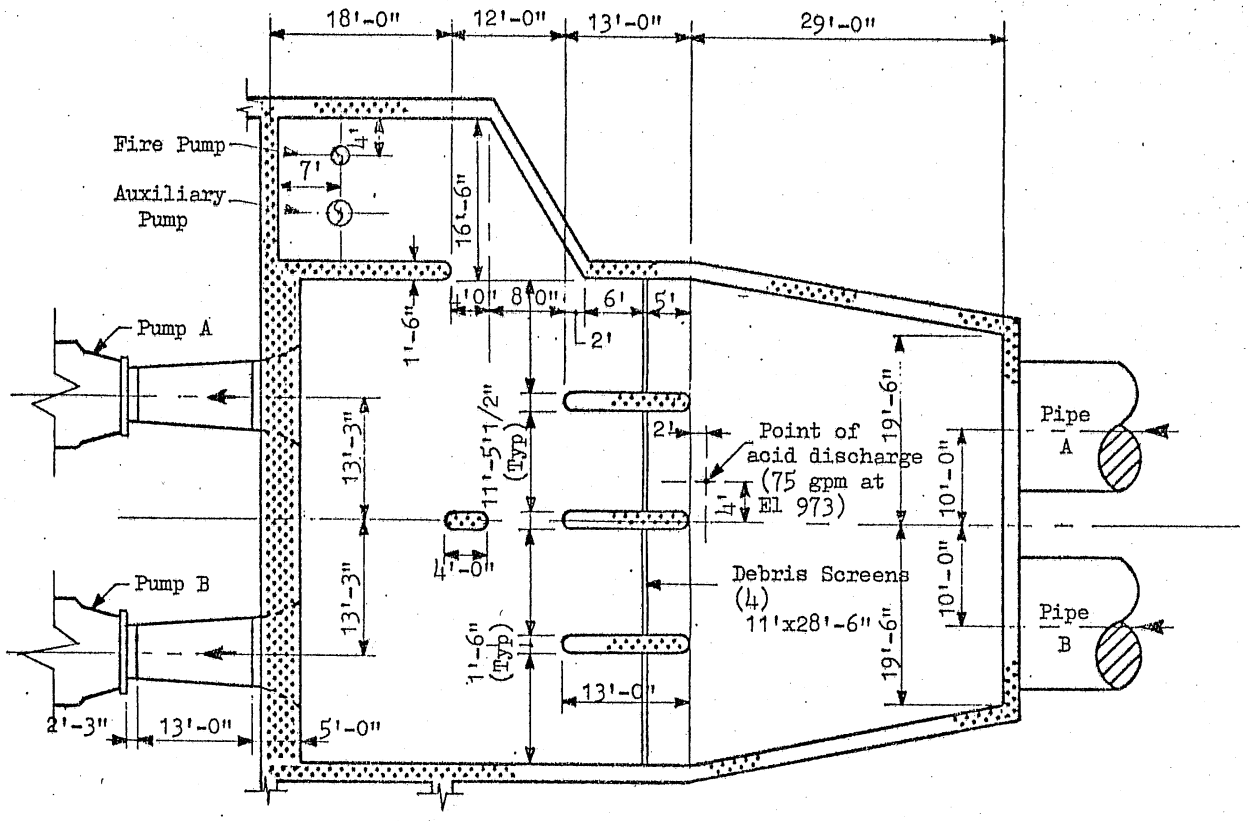

Plan View

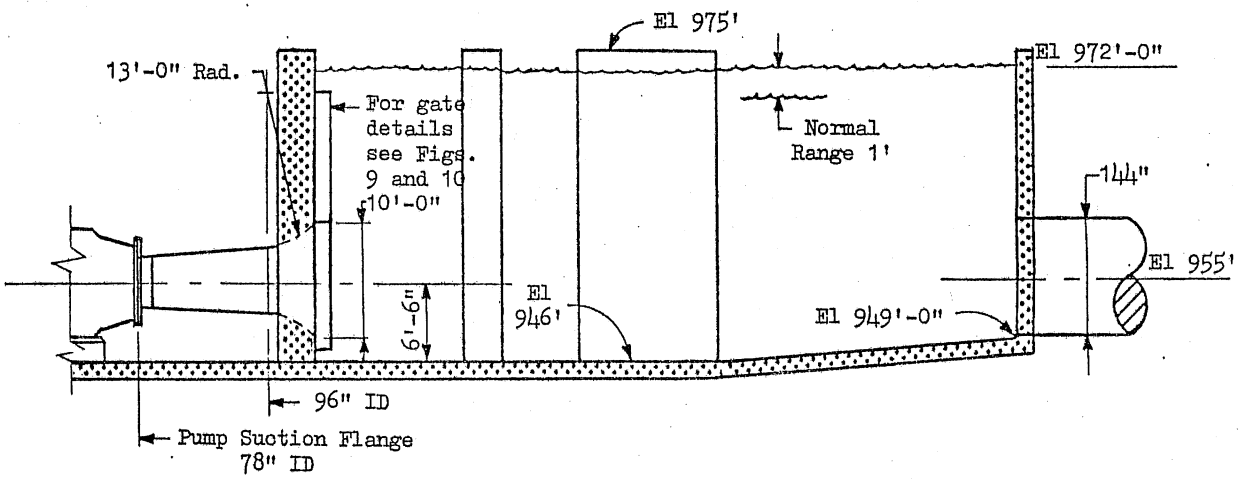

Sectional Elevation

Fig. 7 - Plan and Section Details of the Pump Basin.

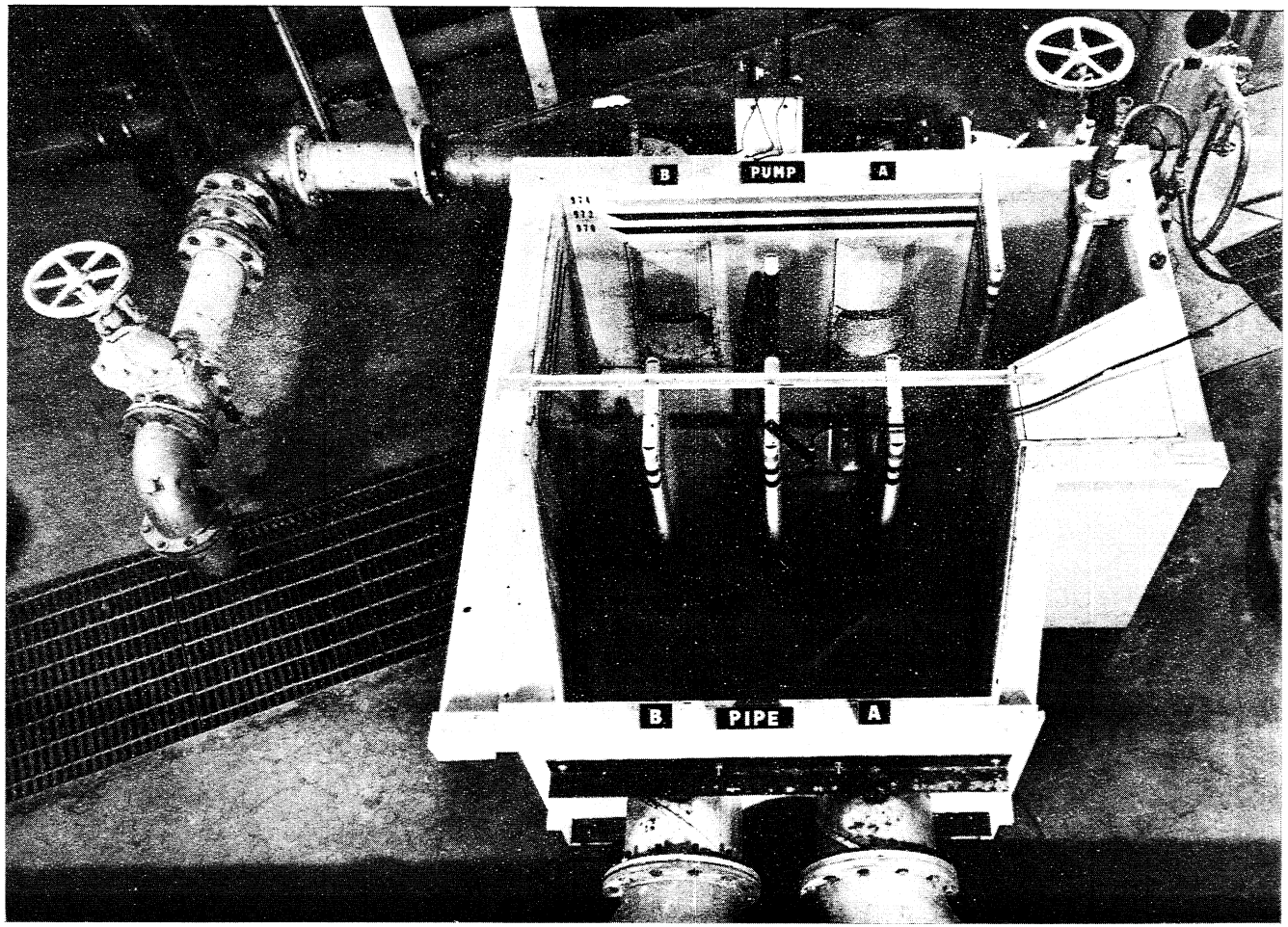

Fig. 8 - The 1:12 Model of the Pump Basin (shown with only one debris screen of 58 percent opening installed).

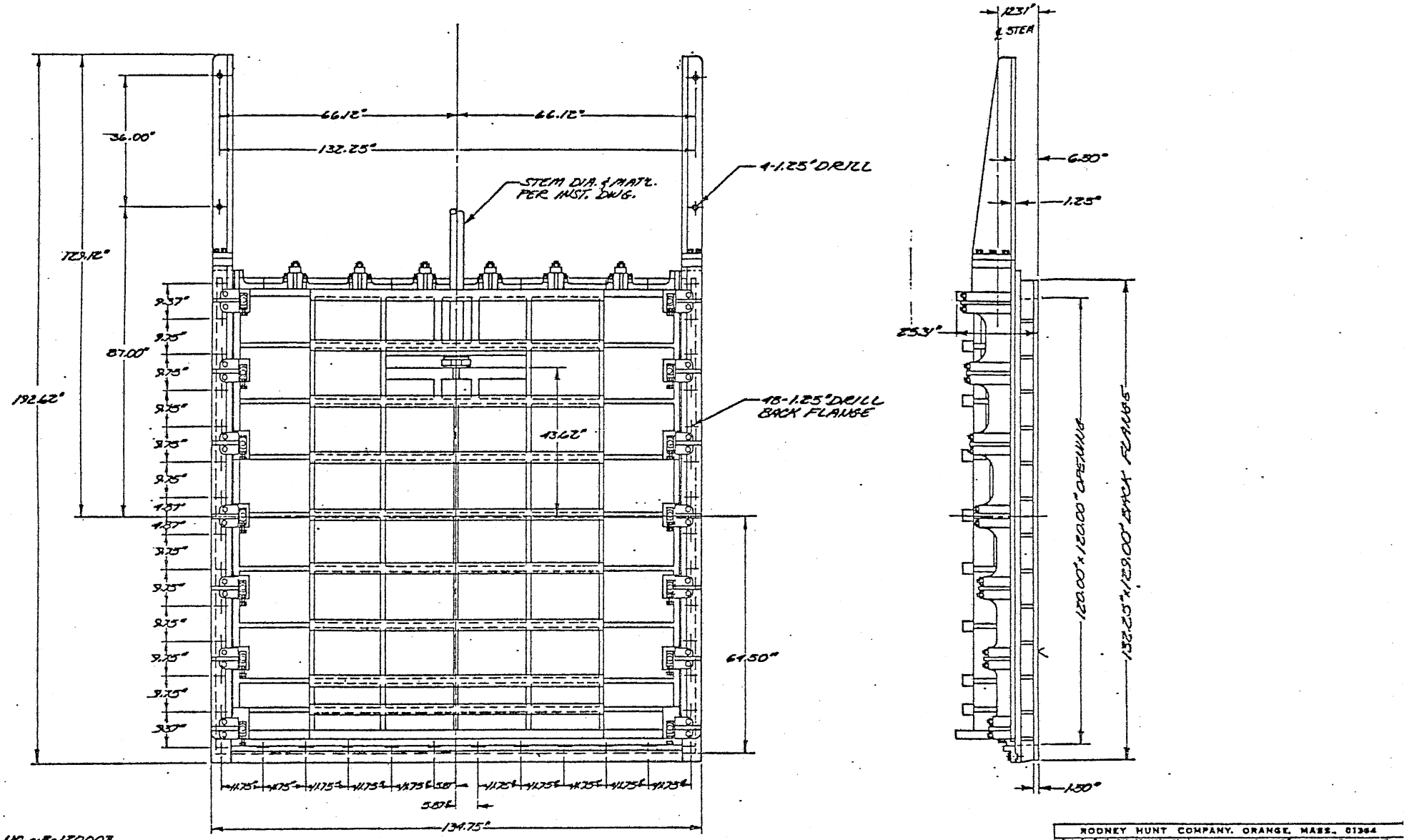

TEMA NO. -B-120003

ALT.	CHANGE	BY	CKD.	DATE	ALT.	CHANGE	BY	CKD.	DATE	ALT.	CHANGE	BY	CKD.	DATE	ALT.	CHANGE	BY	CKD.	DATE	ALT.	CHANGE	BY	CKD.	DATE

FRAME-C-B018 DIST.-C-1301B GUIDE-D-3974 DIT.-D-3975 STOP-E-3618A-6 RET.-E-NCP SEAL-F-4135X TH.UNIT-F-45IPC

RODNEY HUNT COMPANY, ORANGE, MASS., 01364

ASS'Y: 120"x120" SLUICE GATE

SER NAT-Q-120

DRAWN AL | DESIGNED | DATE 11-22-

CHECKED | APPROVED | SCALE 1"=1'-6"

DRAWING SYMBOLS TEA ASP PEA | DRAWER NO. | DWG. NO. C-1-4714

Fig. 9 - Details of the Unwatering Sluice Gate for the Pump Suction.

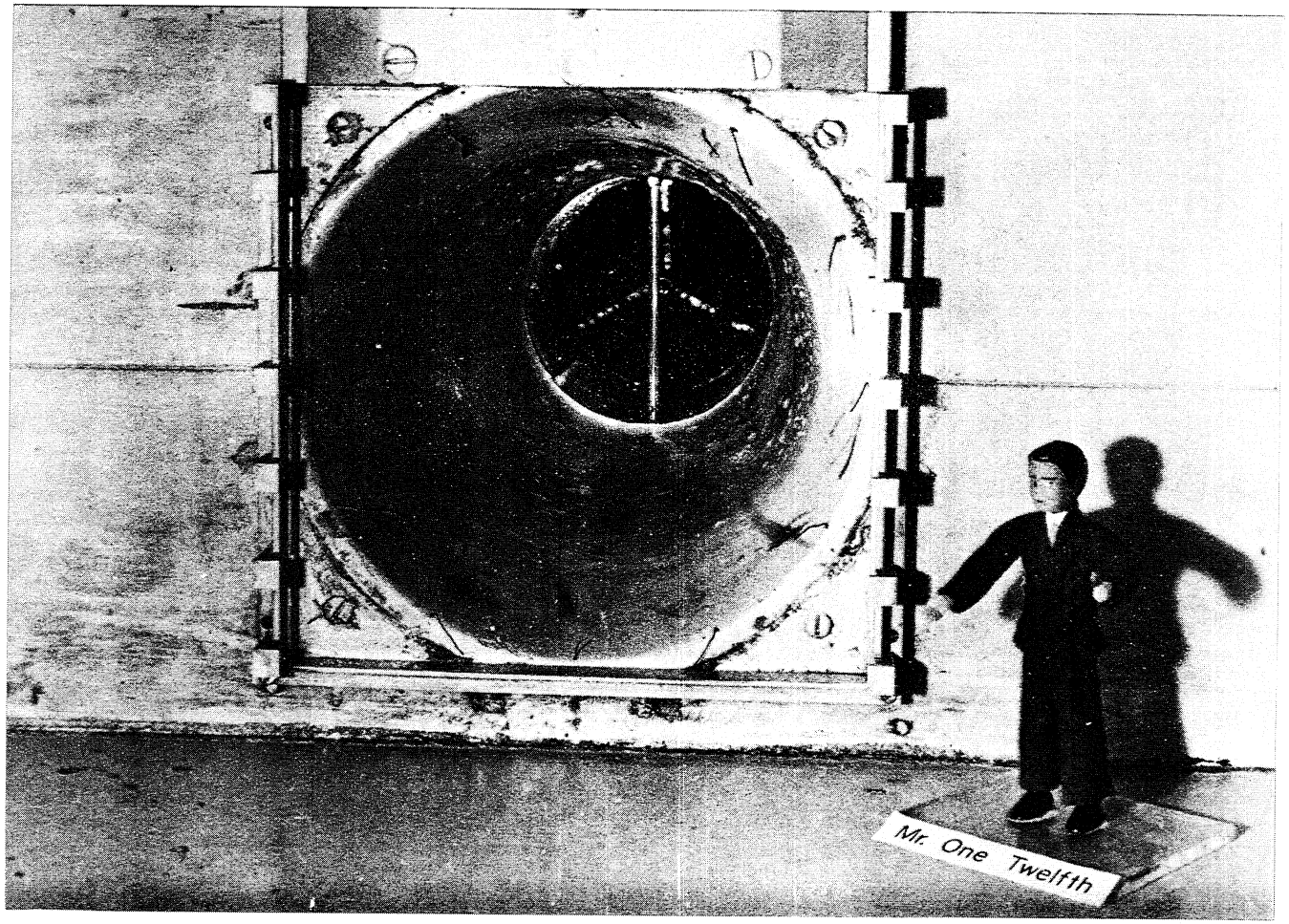

Fig. 10 - The 1:12 Model Simulation of the Pump Suction Intake and Unwatering Sluice Gate (showing flow delineating streamers and gate in open position).

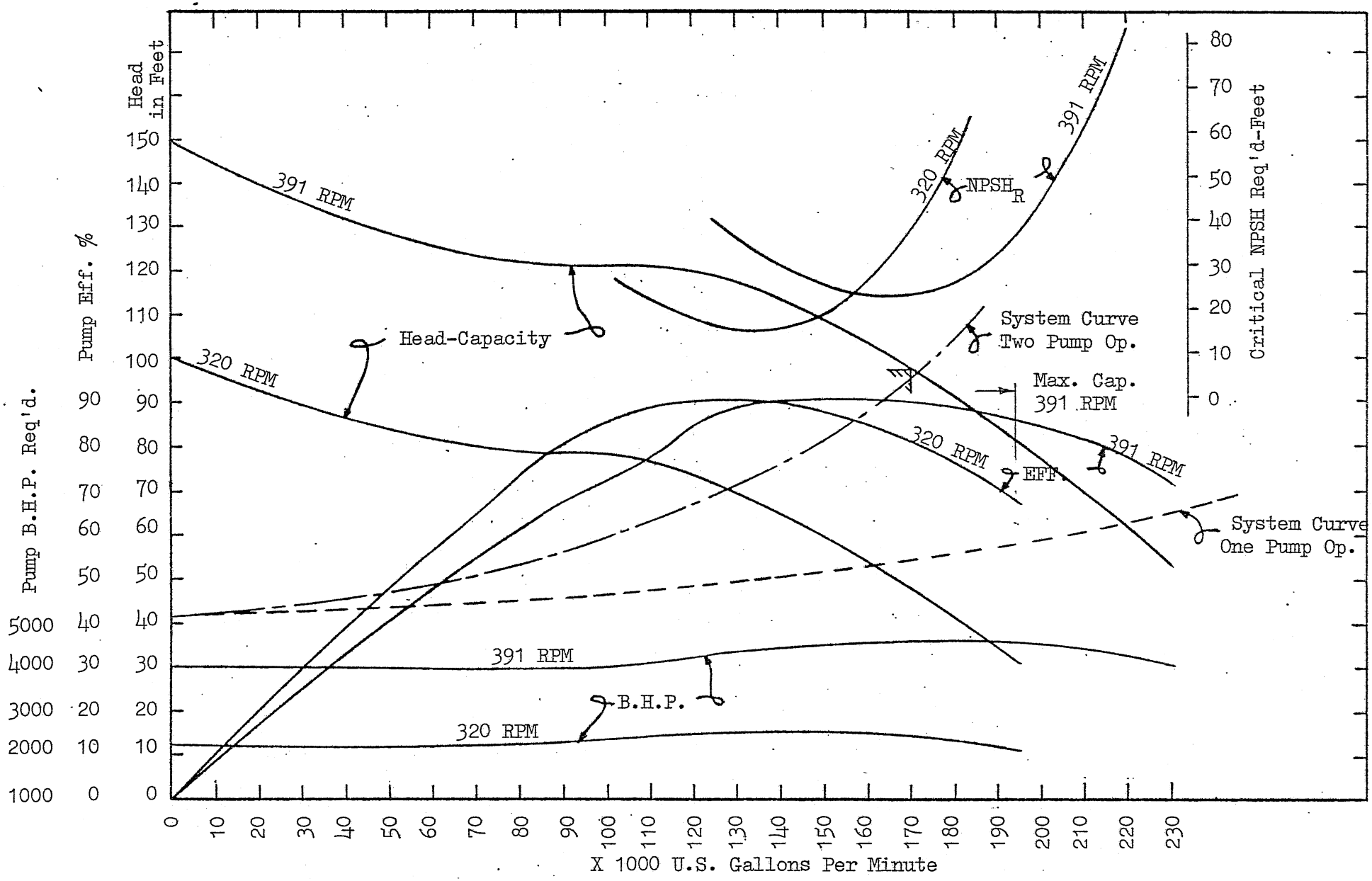

Fig. 11 - Performance Characteristic Curves for Allis-Chalmers 78" x 66" Type WSSD Pump.

Condition (1)	Flow (2) gpm	Pipe (3) A	Pipe (3) B	Pump (3) A	Pump (3) B
1	126,000	X	X	X	X
2	168,000	X	X	X	X
3	79,000	X		X	
4	108,000	X		X	
5	158,000	X		X	
6	79,000	X			X
7	108,000	X			X
8	158,000	X			X
9	158,000	X	X	X	

(1) All the conditions listed in the above table shall be tested assuming a Fire Pump suction of 2000 gpm.

(2) Flow values are full-scale and are per pump and/or per tower.

(3) Refer to Fig. 7 for pipe and pump locations.

Fig. 12 - Test Conditions Required to be Examined in the Model.

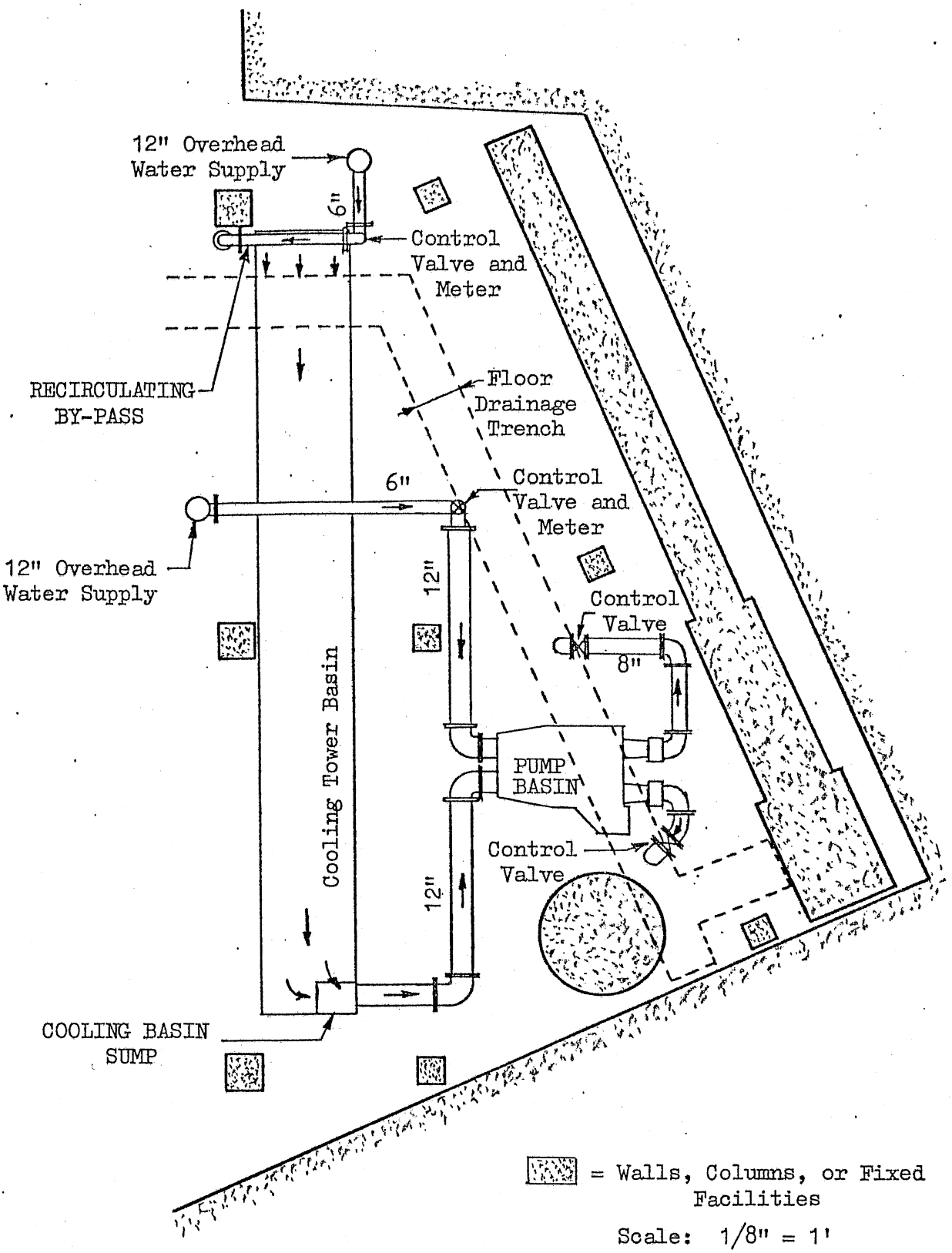

Fig. 13 - Laboratory Layout for the 1:12 Scale Model.

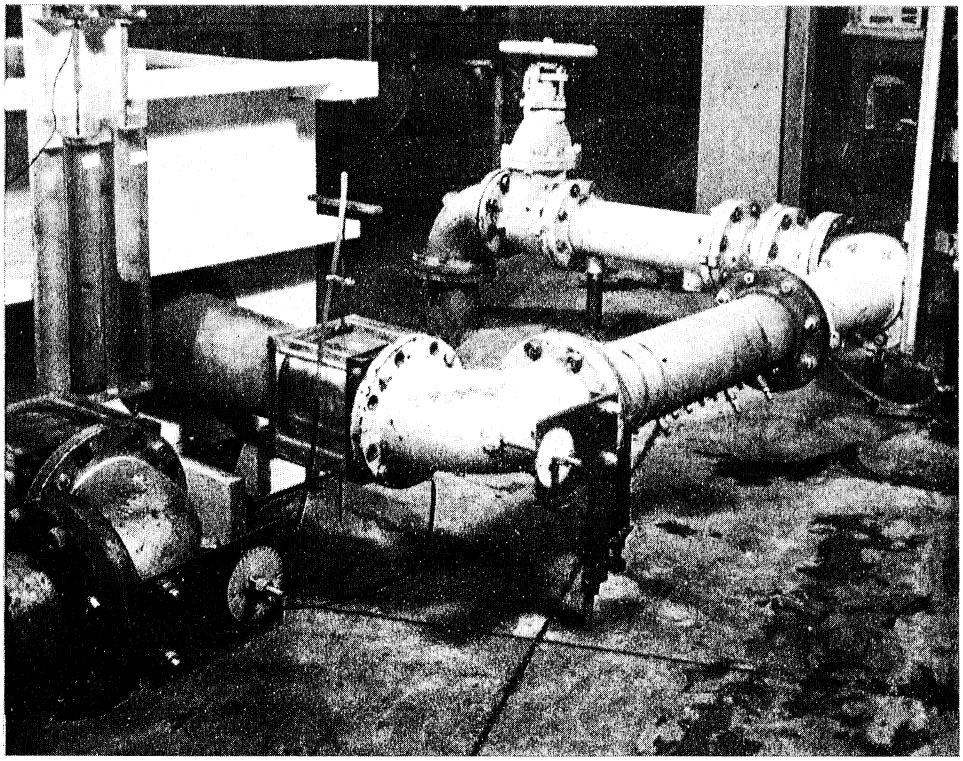

Fig. 14 - The Pump Basin Discharge System.

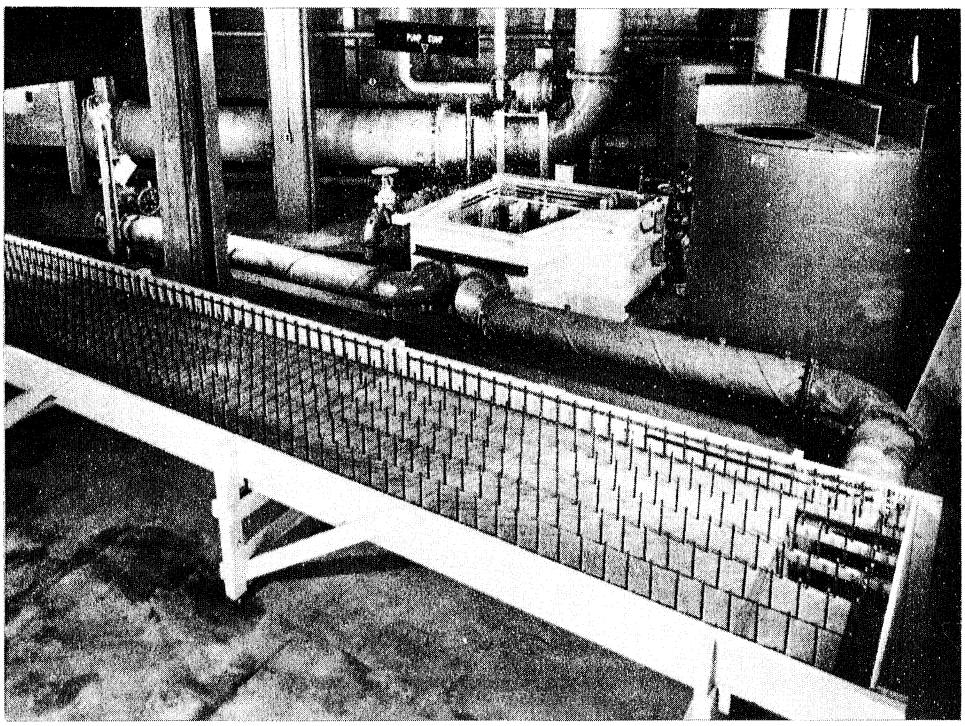

Fig. 15 - The Cooling Tower Basin, Basin Sump and Pump Basin.

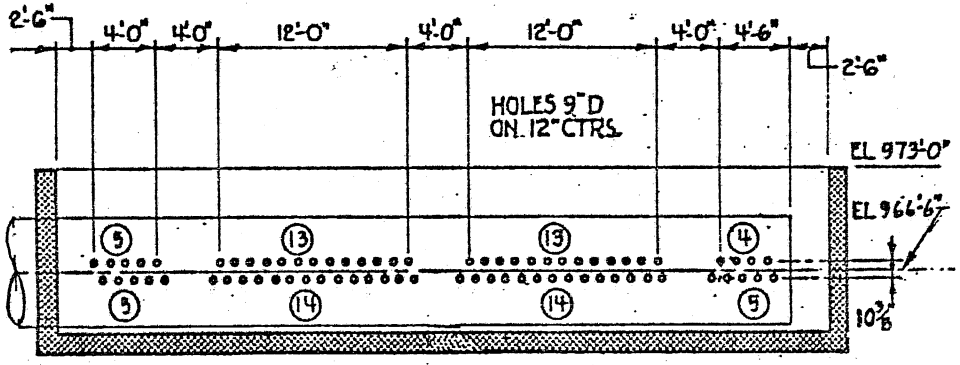

(a) Original Hole Pattern

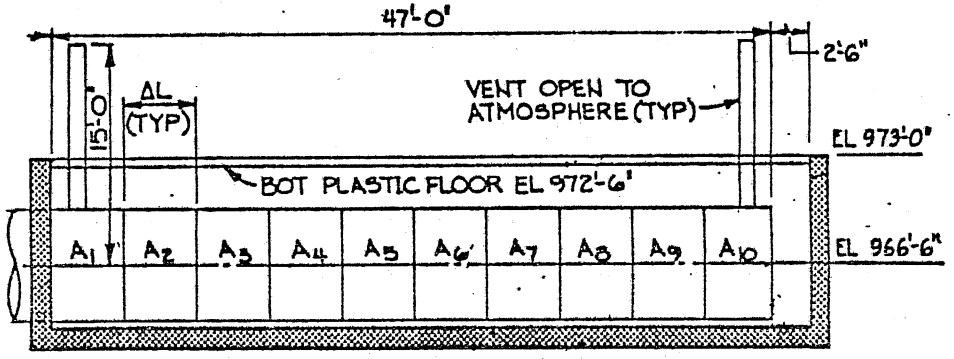

(b) Revised Hole Pattern-Section Arrangement

SECTION	HOLE PATTERN (BY HOLE NUMBER)
A_1	1-17
A_2	2-16
A_3	1,3,4,6-13,15-17
A_4	1-3, 5, 7-9, 11, 13-15, 17
A_5	1-3, 5, 7-9, 11, 13-15
A_6	1,3,4,6,7,9,10,12,13,15
A_7	1,3,4,6,7,9,10,12,13,15
A_8	1,3,5,7,9,11,13,15,17
A_9	1,3,5,7,9,11,13,15,17
A_{10}	1,3,6,8,10,13,15,17

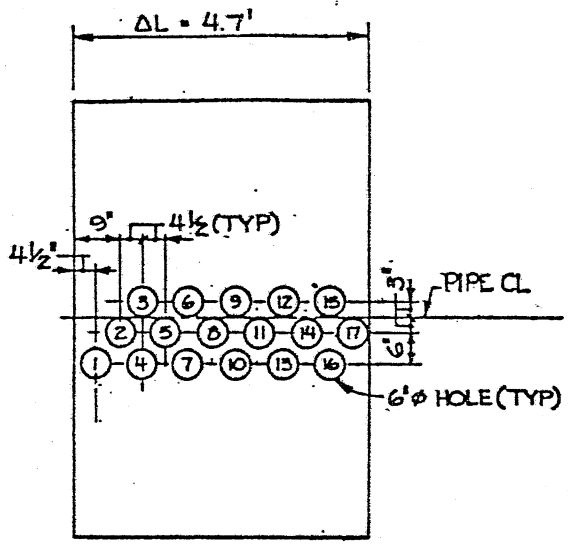

(c) Revised Hole Pattern-Hole Arrangement in Sections

Fig. 16 - Hole Arrangement for Manifold Pipe.

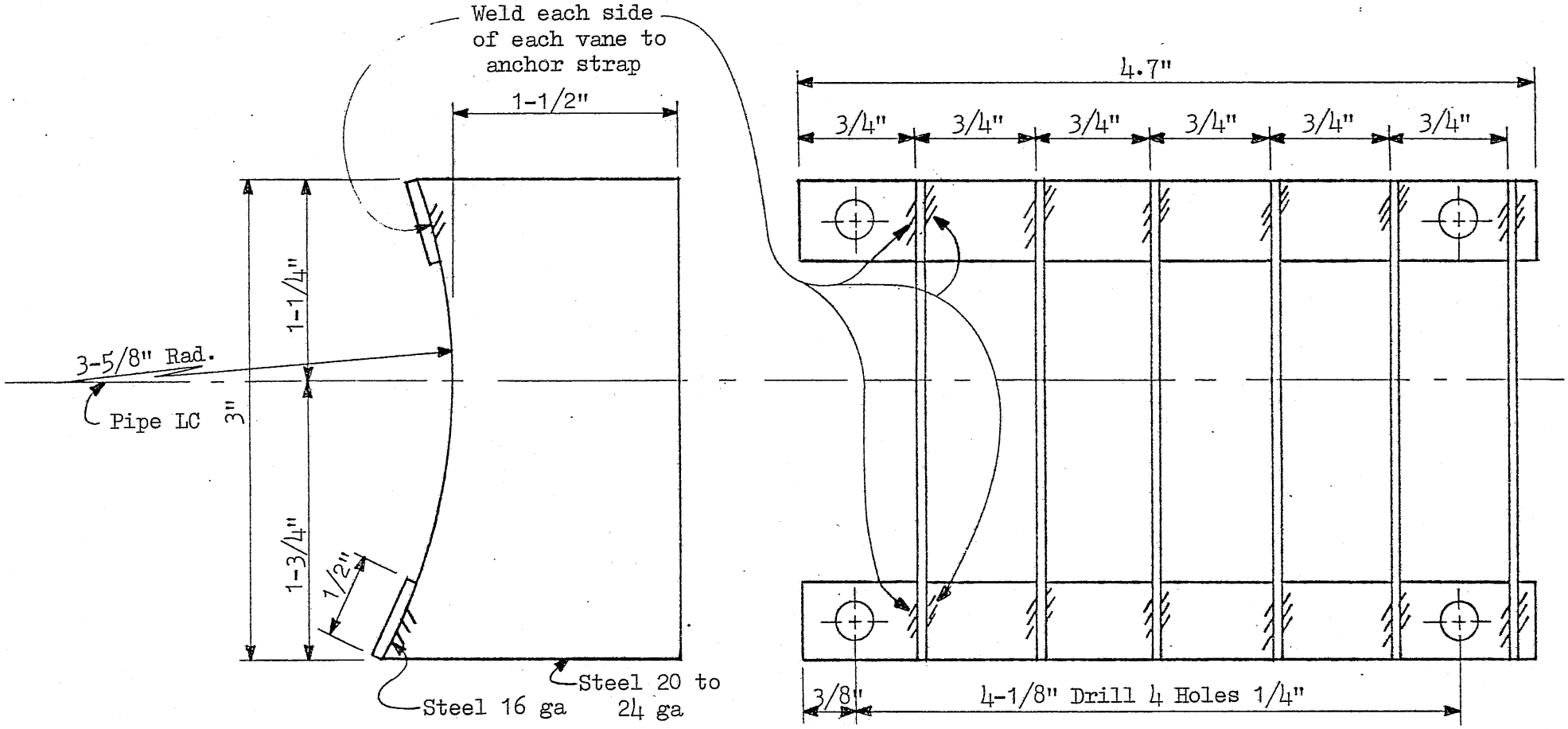

Note: Make 10 units. Position each valve unit to fit each 4.7" unit length which is shown as A, thru A_{10} in Fig. 16.
Dimensions on this drawing gave for the model.

Fig. 17 - Details of the Manifold Flow Straightening Vanes as Used in the Revised Manifold Model.
(dimensions shown are for the model)

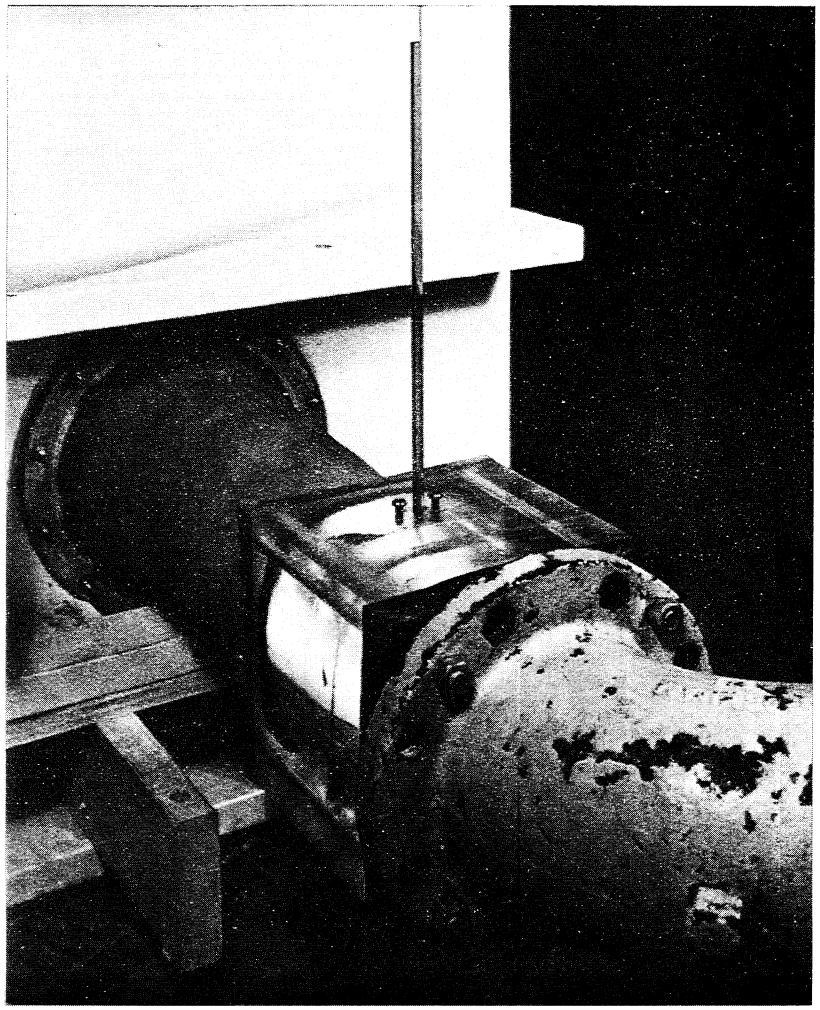

Fig. 18 - Arrangement for Measuring Boundary Pressure Fluctuations at the Pump Suction.

Fig. 19 - The Rotatable Vortex Sensor Assembly.

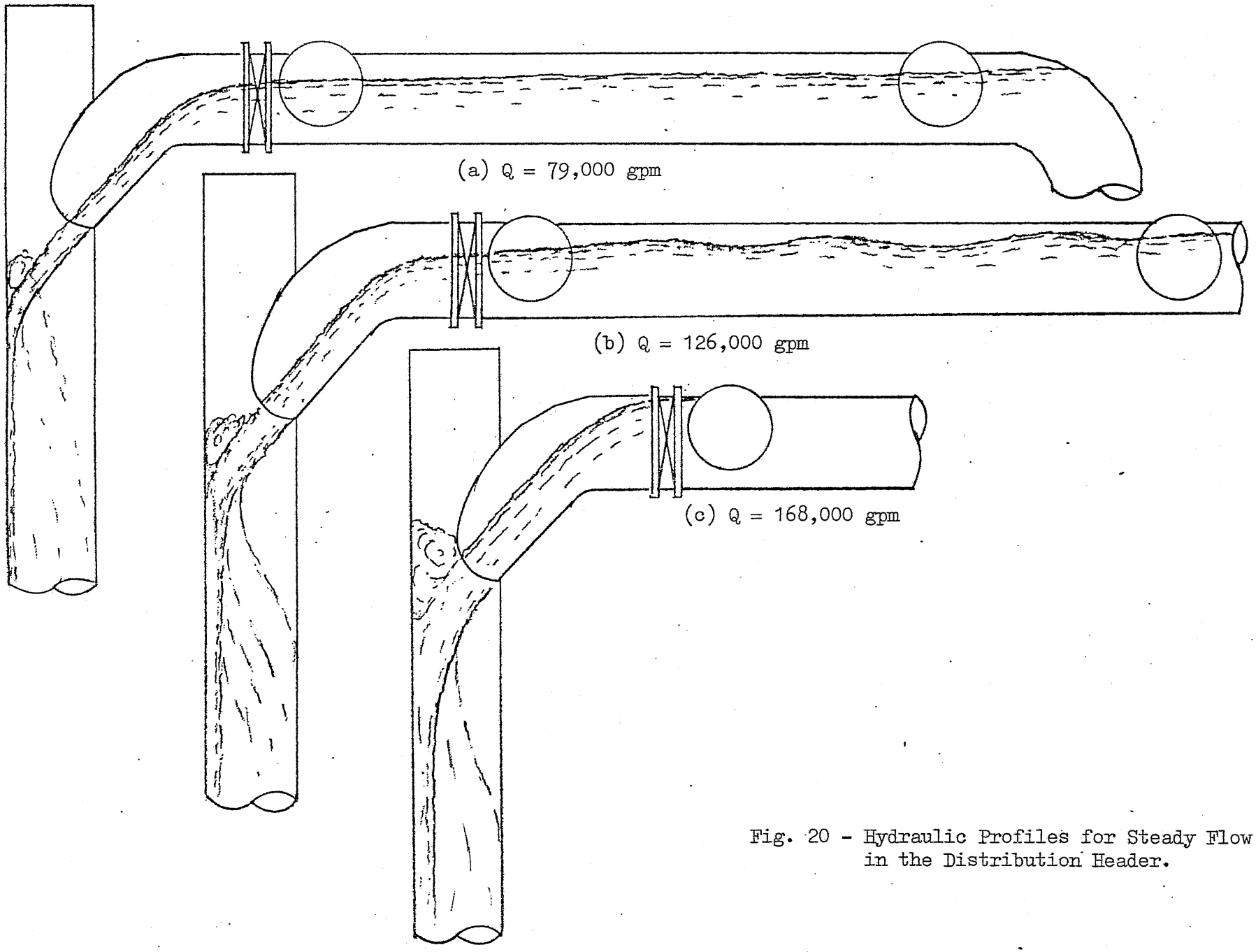

Fig. 20 - Hydraulic Profiles for Steady Flow in the Distribution Header.

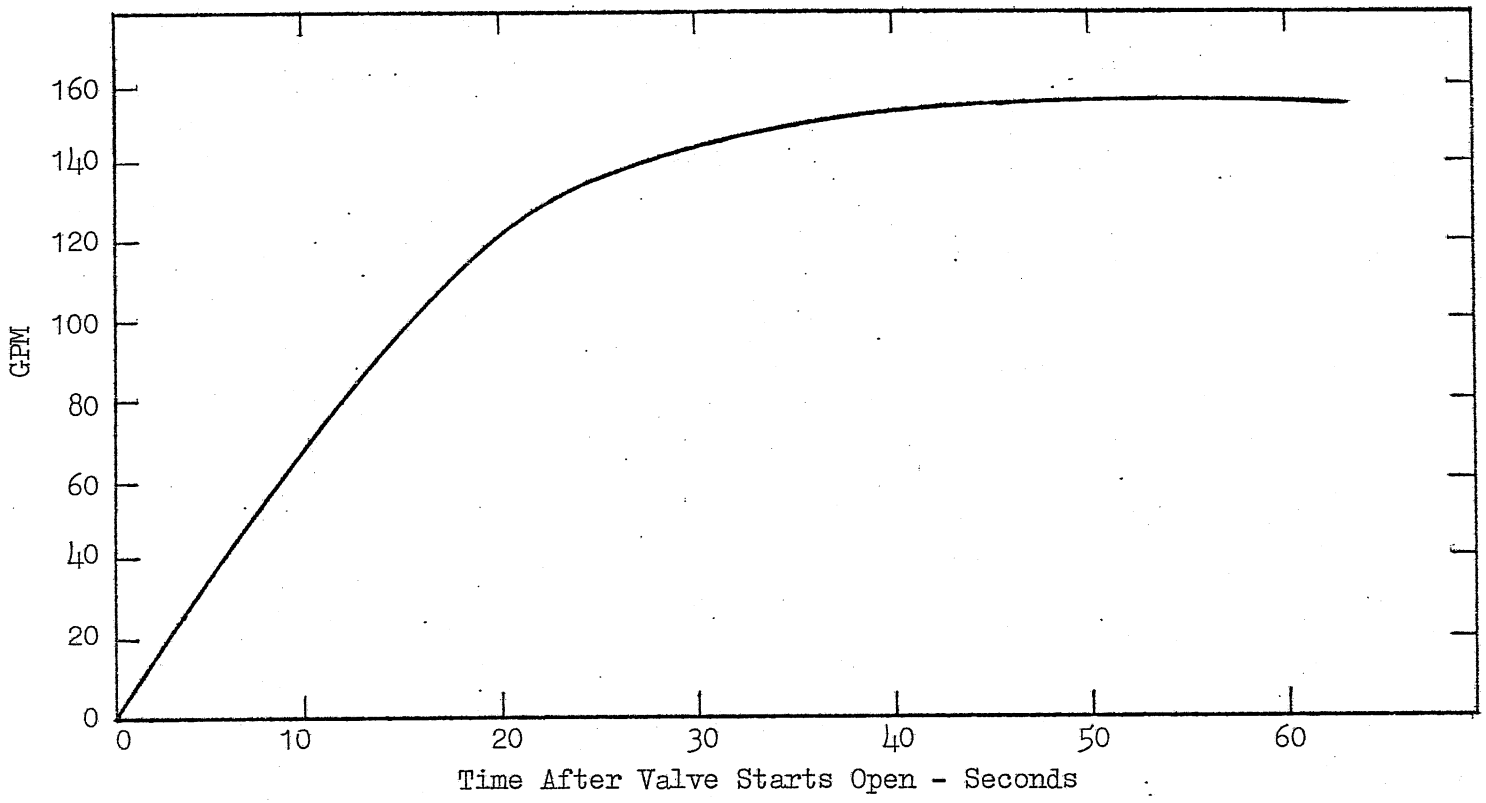

Fig. 21 - Estimated Time-Discharge Curve for the Pumping Station at Startup - One Pump, Low Speed.

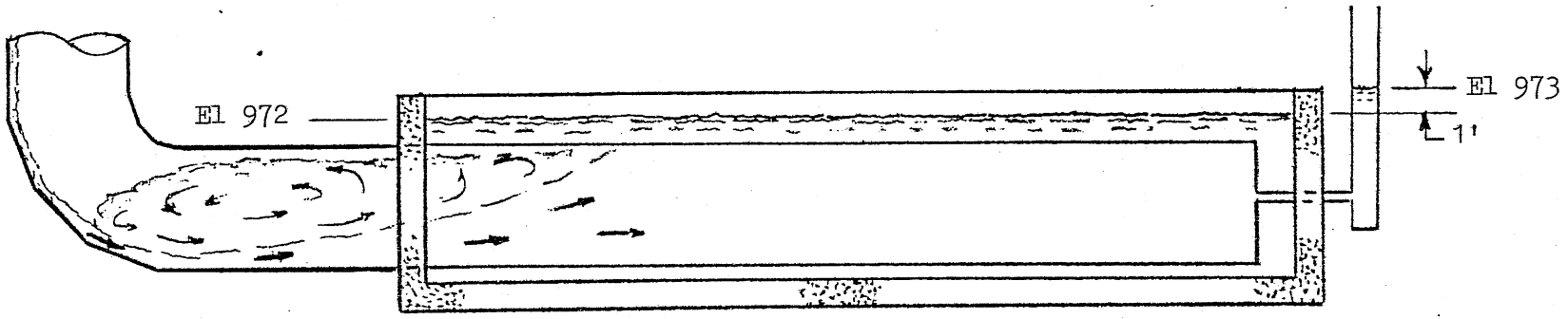

(a) Q_{fs} = 79,000 gpm

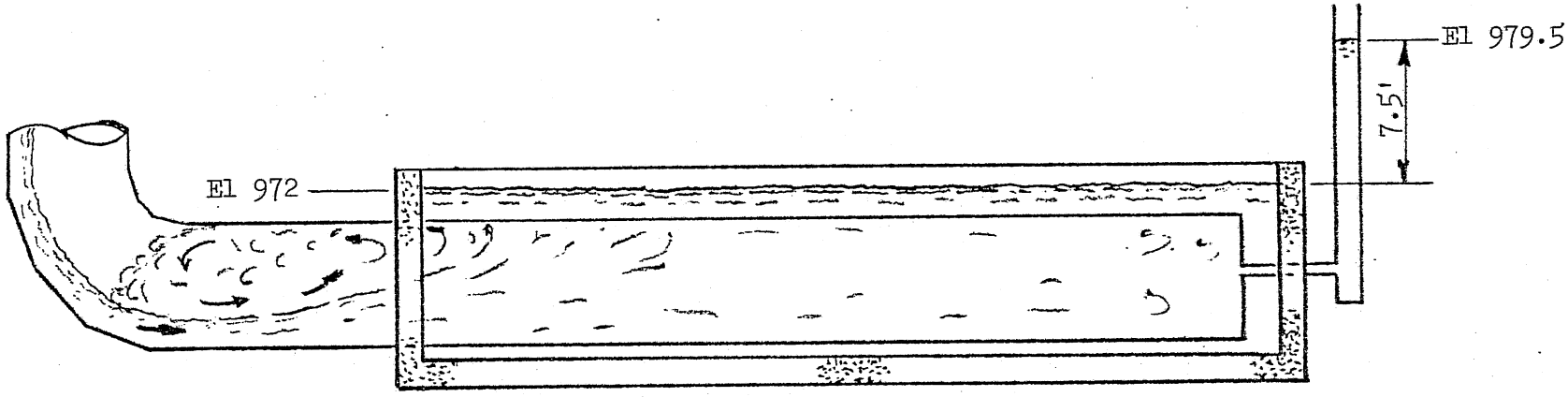

(b) Q_{fs} = 168,000 gpm

Fig. 22 - Flow Character in the Lower Elbow and Manifold with the Original Hole Arrangement.

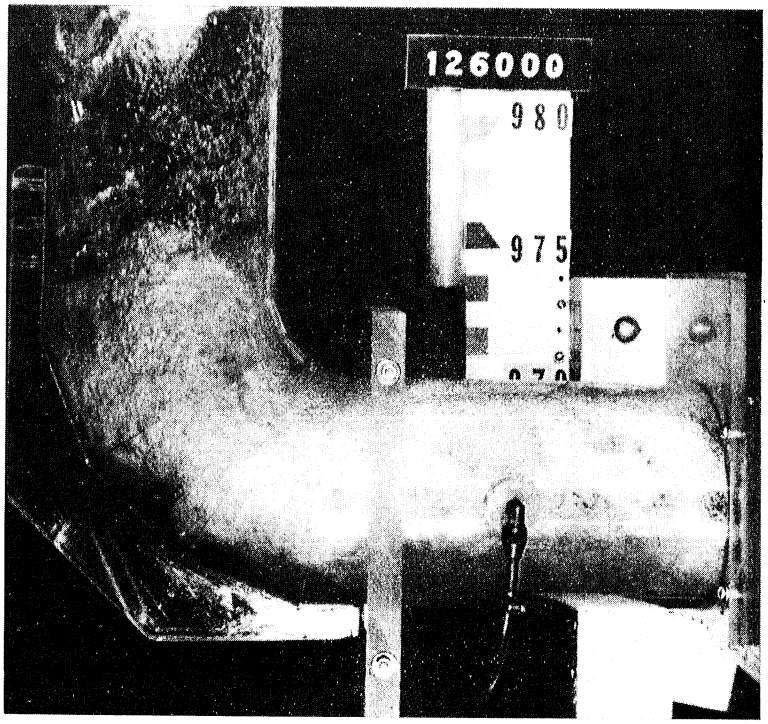

(a) Q_{fs} = 126,000 gpm

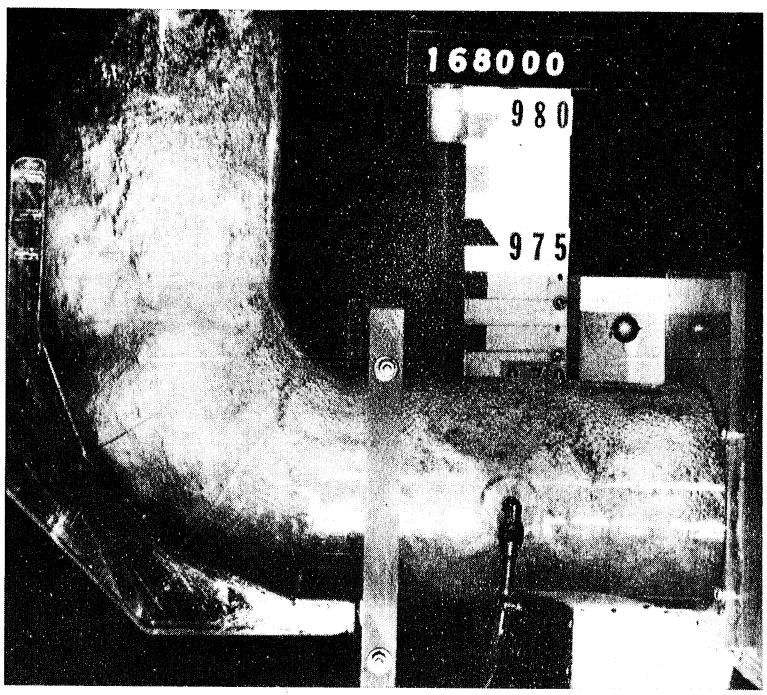

(b) Q_{fs} = 168,000 gpm

Fig. 23 - Flow Character in the Lower Elbow with the Revised Manifold Arrangement.

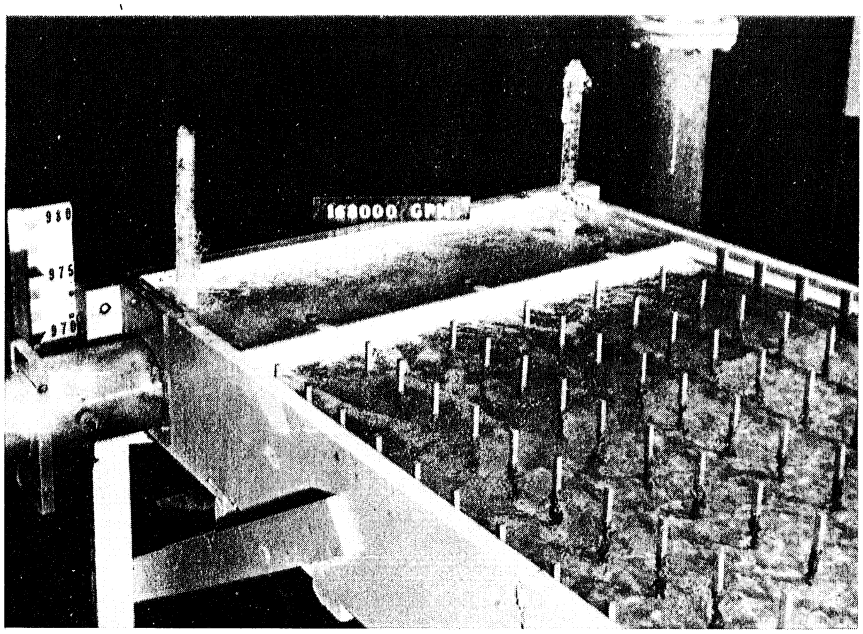

(a) Perspective View

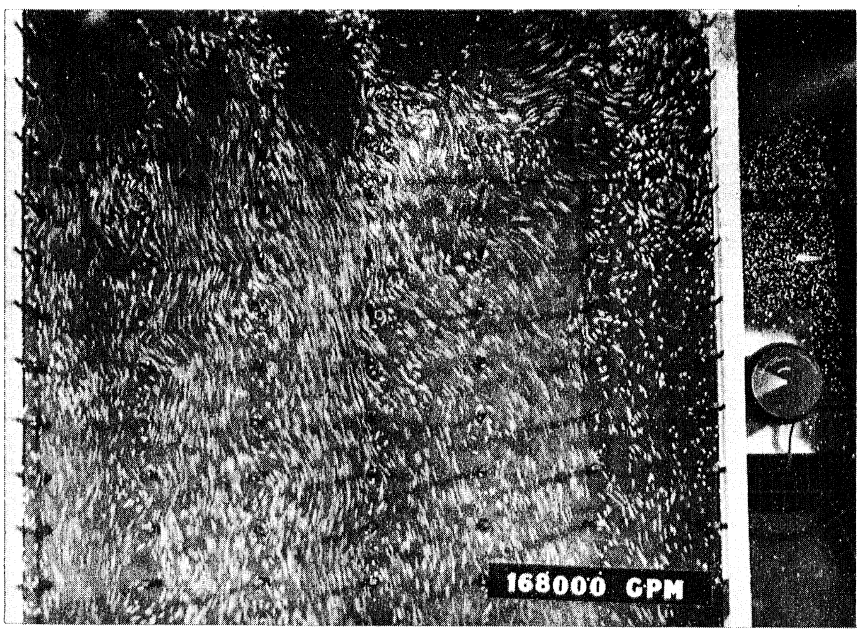

(b) Plan View with Surface Confetti

Fig. 24 - Flow Character in the Manifold Vent Stacks and Basin Entrance with the Revised Manifold and Full Vaning (Q = 168,000 gpm).

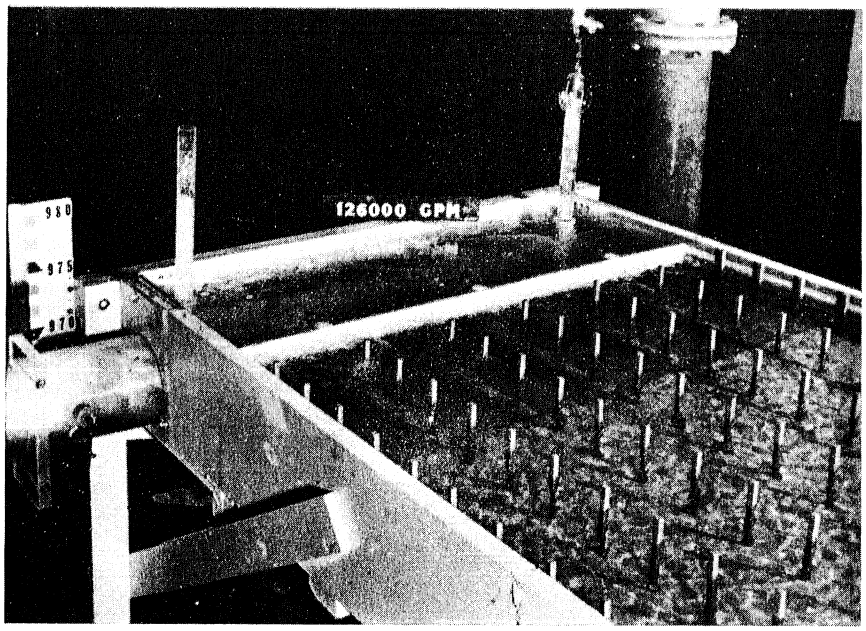

(a) Perspective View

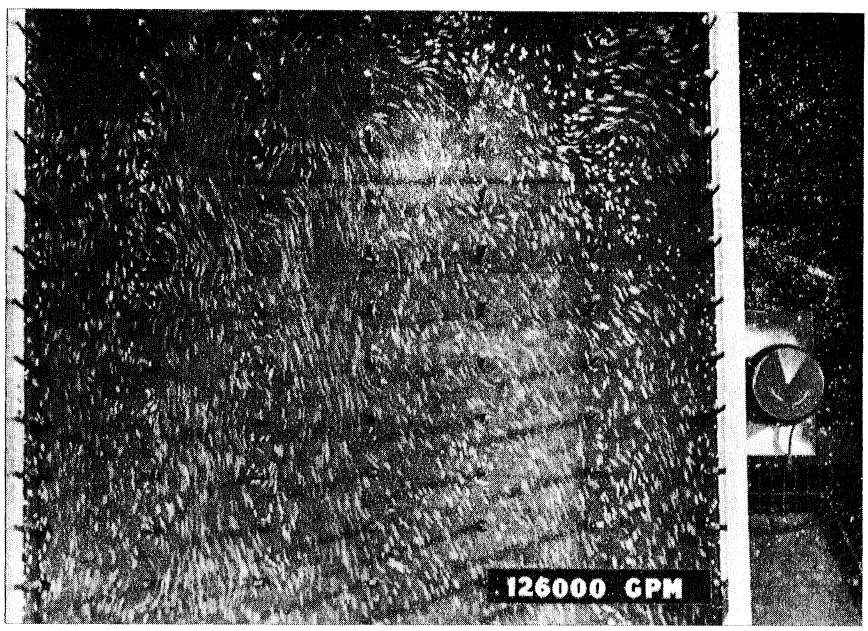

(b) Plan View with Surface Confetti

Fig. 25 - Flow Character in the Manifold Vent Stacks and Basin Entrance with the Revised Manifold and Full Vaning (Q = 126,000 gpm).

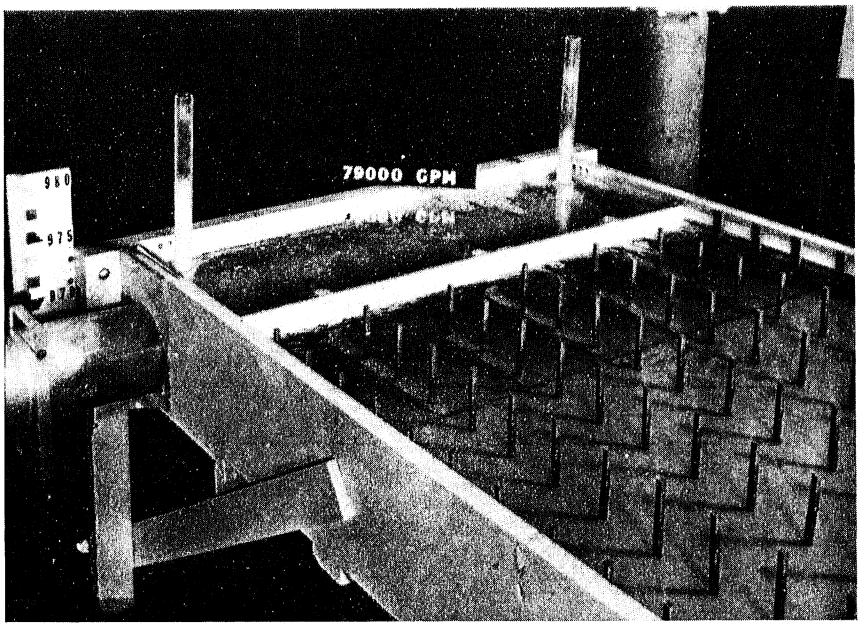

(a) Perspective View

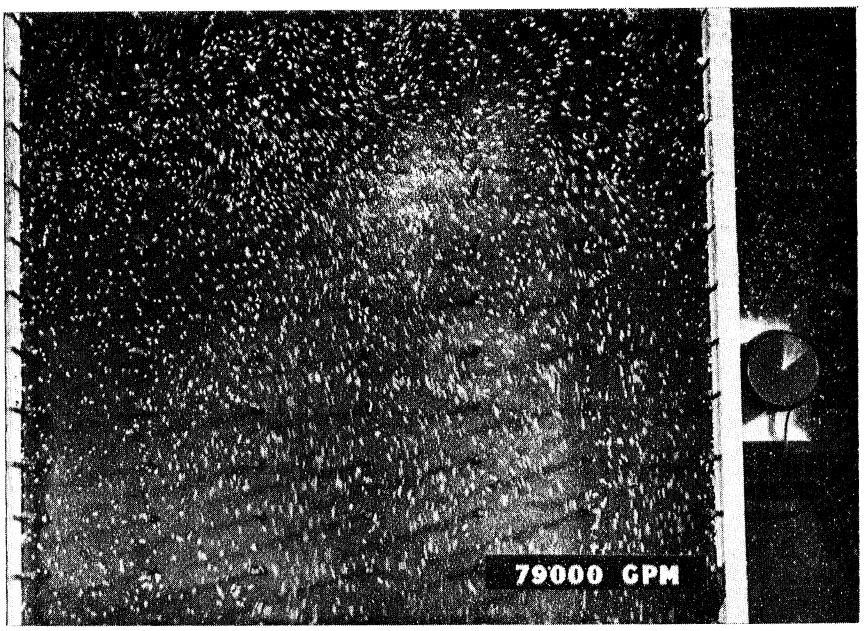

(b) Plan View with Surface Confetti

Fig. 26 - Flow Character in the Manifold Vent Stacks and Basin Entrance with the Revised Manifold and Full Vaning (Q = 79,000 gpm).

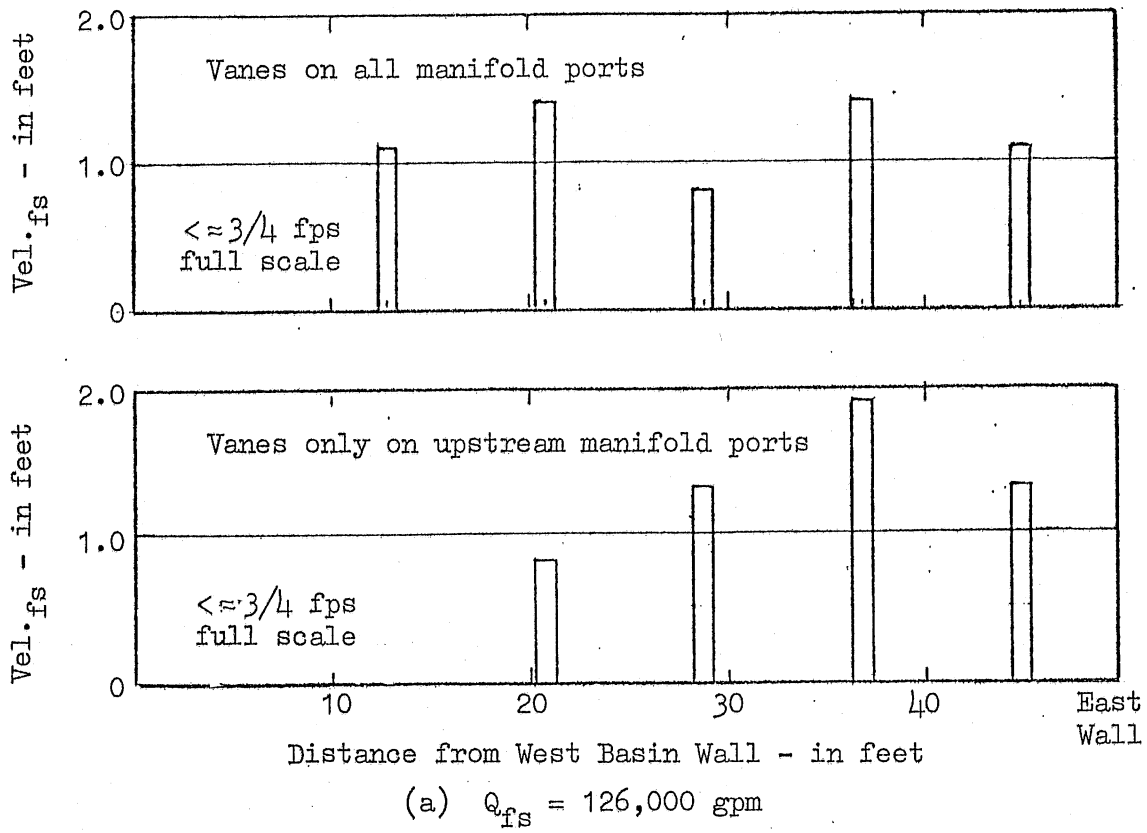

(a) Q_{fs} = 126,000 gpm

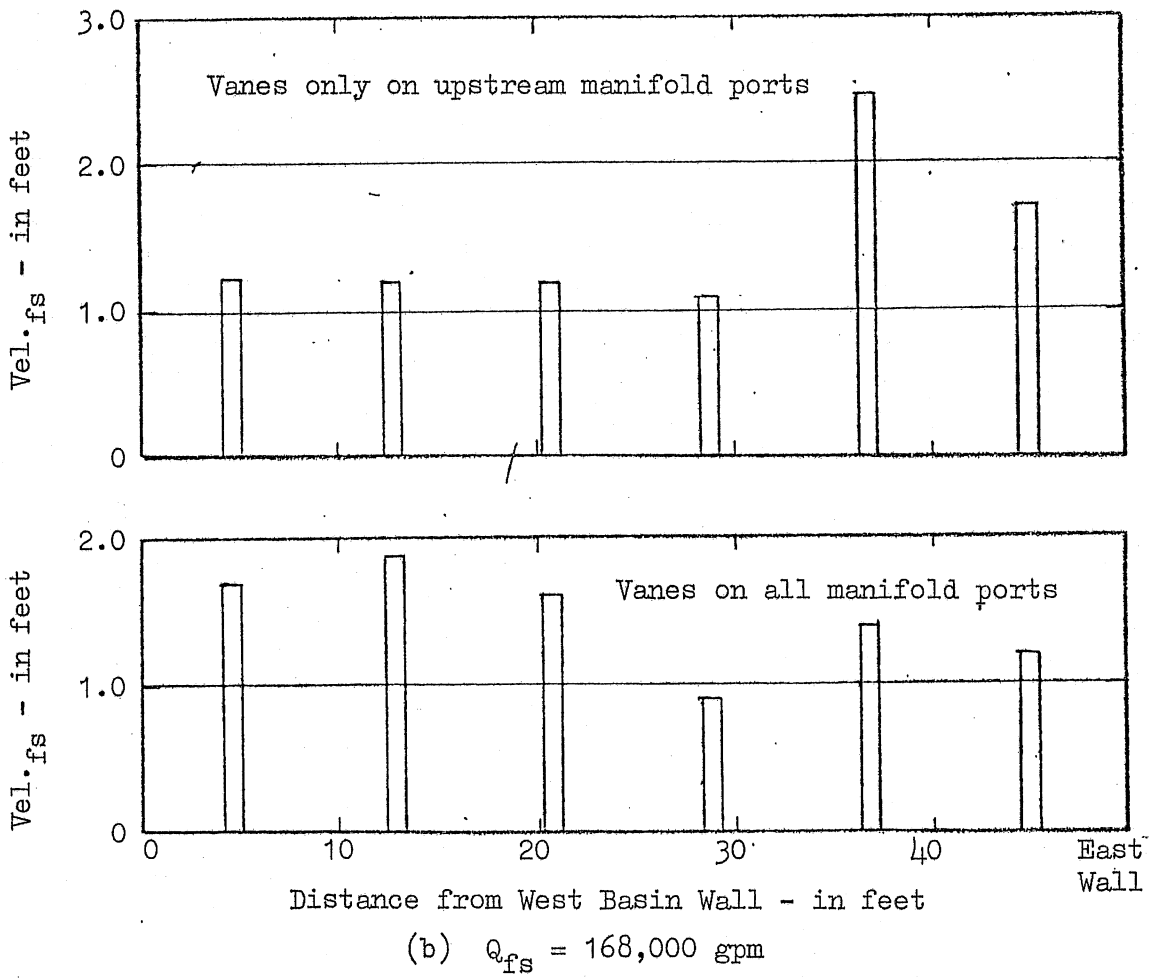

(b) Q_{fs} = 168,000 gpm

Fig. 27 - Velocity Distribution in the Cooling Tower Basin at a Section Fifteen Feet Downstream of the Floor Ramp.

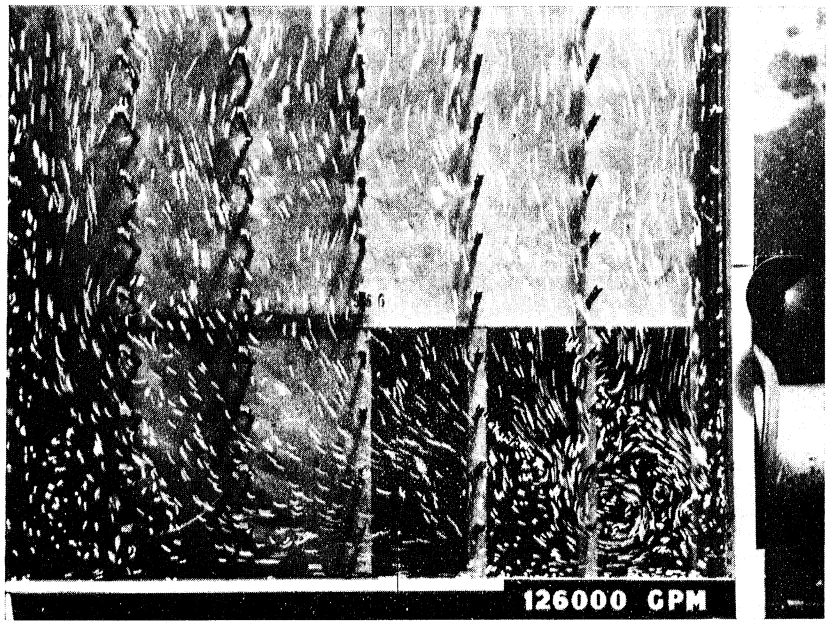

(a) Q_{fs} = 126,000 gpm

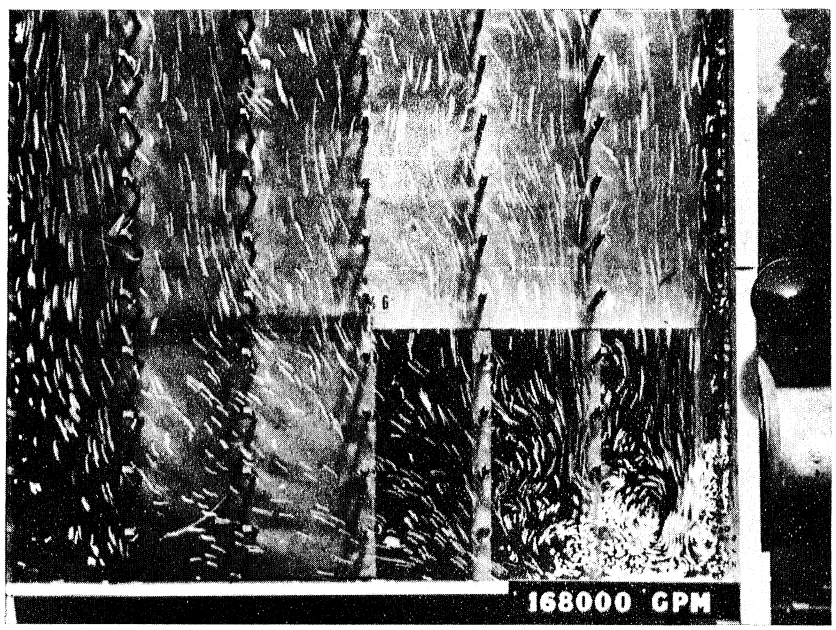

(b) Q_{fs} = 168,000 gpm

Fig. 28 - Surface Flow Character in the Cooling Basin Sump as Shown by Floating Confetti.

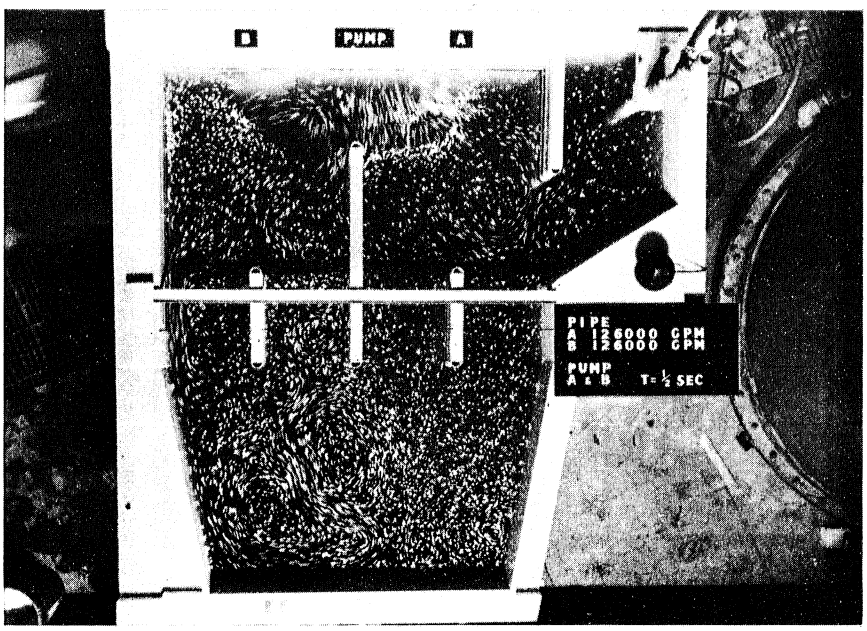

(a) Q = 126,000 gpm

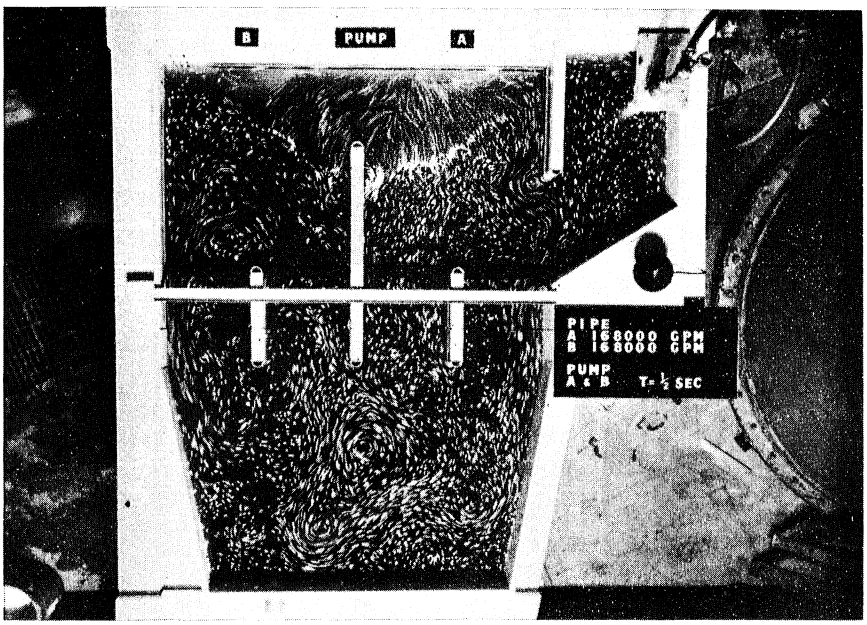

(b) Q = 168,000 gpm

Fig. 29A - Surface Flow Character in the Pump Basin as Shown by Floating Confetti - Two Pumps Operating.

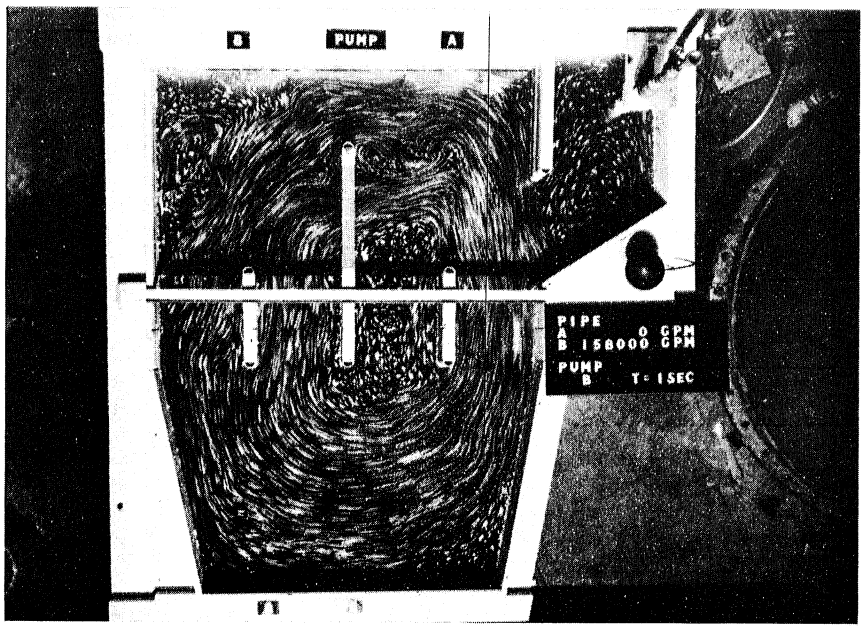

(a) Q = 158,000 gpm without resisting trash screens

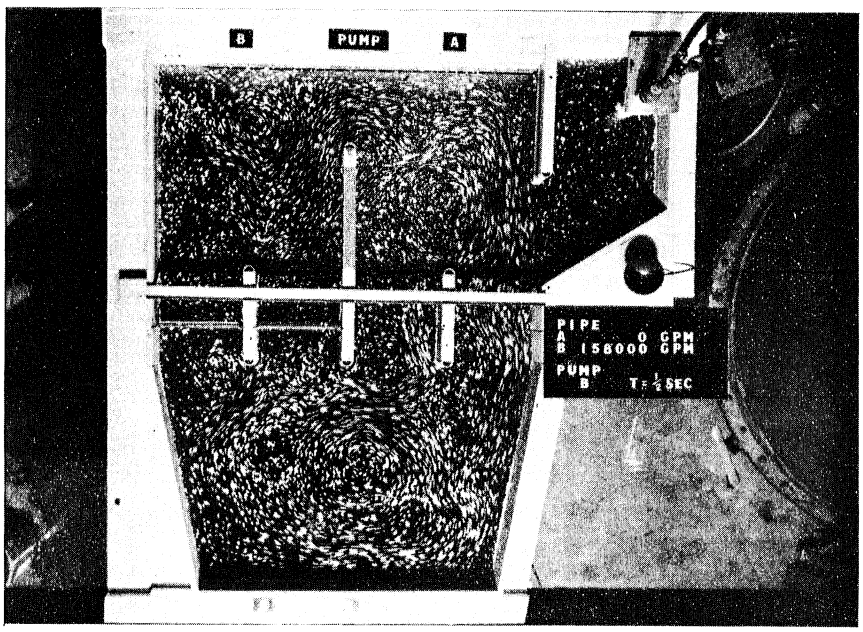

(b) Q = 158,000 with resisting trash screens on the flow route

Fig. 29B - Surface Flow Character in the Pump Basin as Shown by Floating Confetti - One Pump Operating - Flow Aligned.

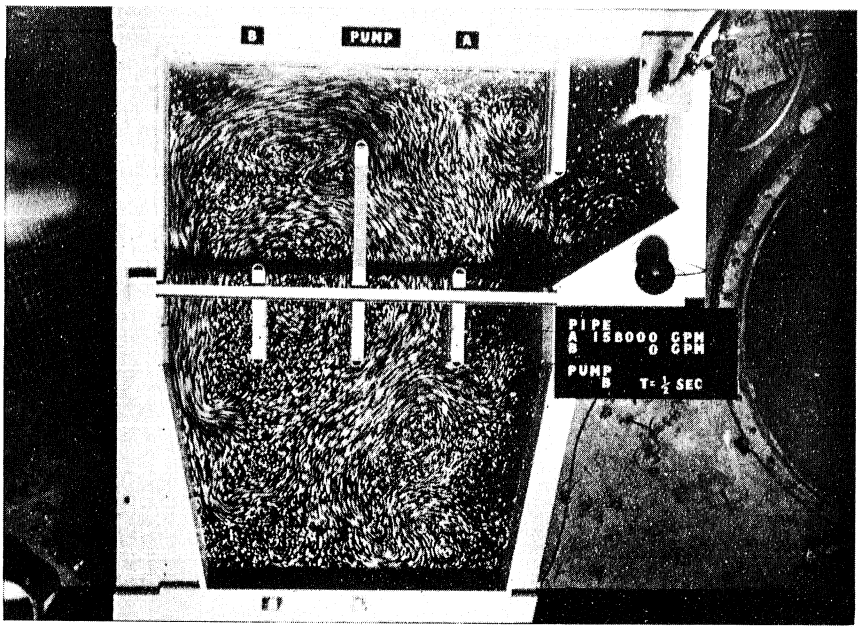

(a) Q = 158,000 gpm without resisting trash screens

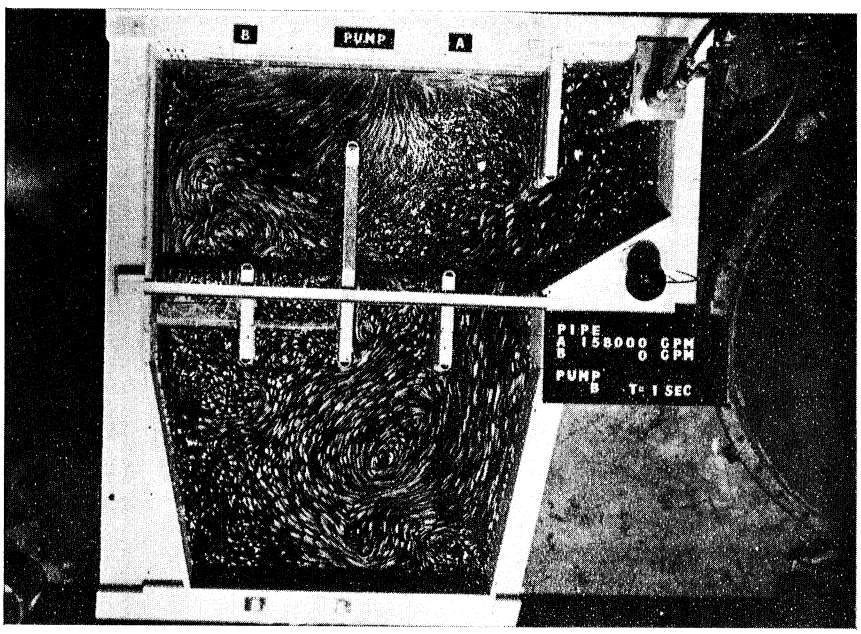

(b) Q = 158,000 gpm with resisting trash screens

Fig. 29C - Surface Flow Character in the Pump Basin as Shown by Floating Confetti - One Pump Operating - Flow Not Aligned.

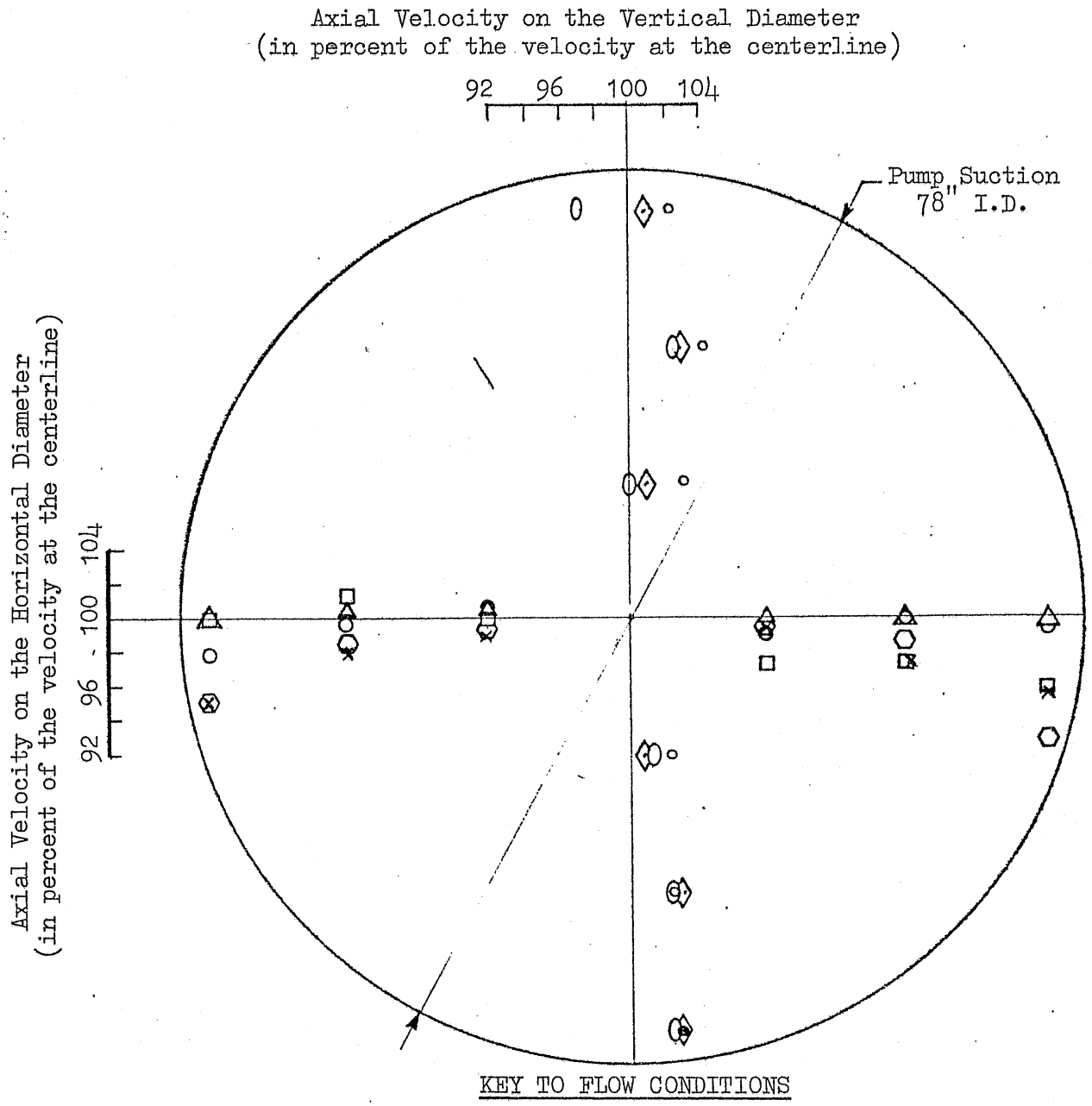

KEY TO FLOW CONDITIONS

	Symbol	Pipes Flowing (in gpm) A	Pipes Flowing (in gpm) B	Pumps Operating A	Pumps Operating B
Horiz.	⊡	79,000	-	-	X
	×	158,000	-	-	X
	⊙	158,000 (2 east screens + fire pump)		-	X
	△	126,000	126,000	X	X
	⊙	168,000	168,000	X	X
Vert.	⊙	168,000	168,000	X	X
	◇	126,000	-	X	-
	0	79,000	-	X	-

Fig. 30 - Velocity Profiles for Flow Entering the Pump Suctions.

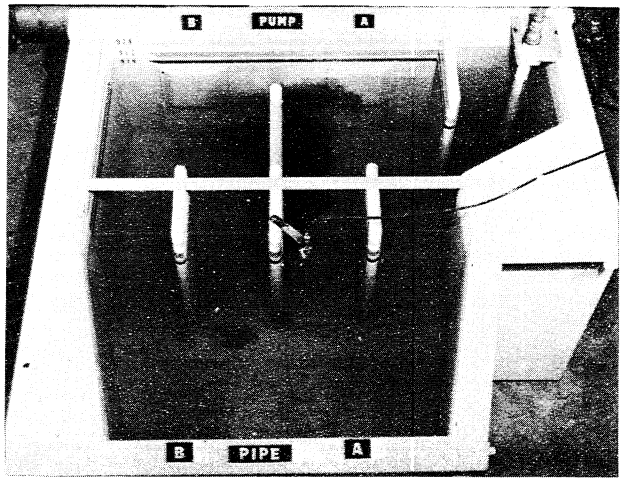

(a) 11 secs. (38 secs. full scale) after starting injection

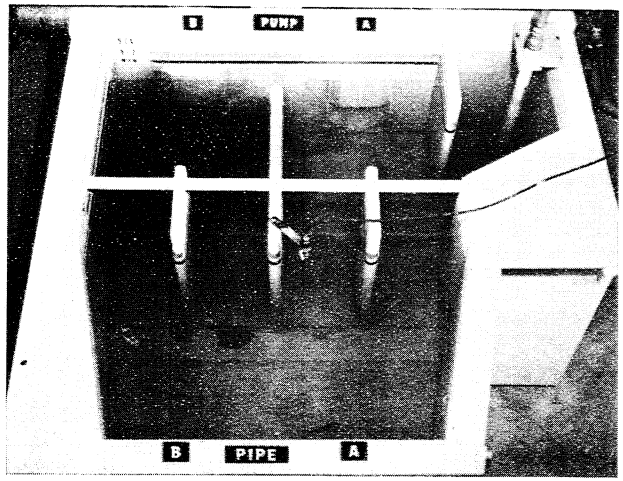

(b) 20 secs. (69 secs. full-scale) after starting injection

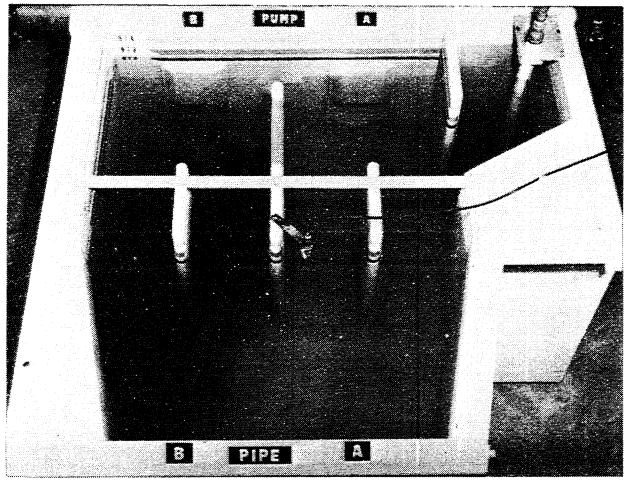

(c) 30 secs. (104 secs. full-scale) after starting injection

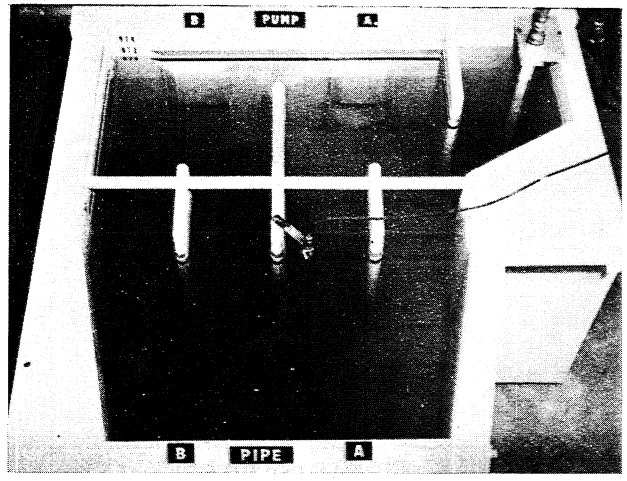

(d) 40 secs. (138 secs. full-scale) after starting injection

Fig. 31 - Dye Simulated Flow Patterns for Acid Injection in the Pump Basin with Pipe A Flowing to Pump A.

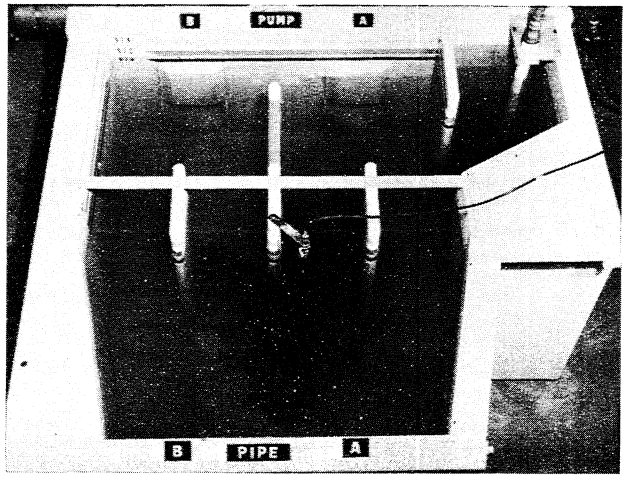

(a) 11 secs. (38 secs. full scale) after starting injection

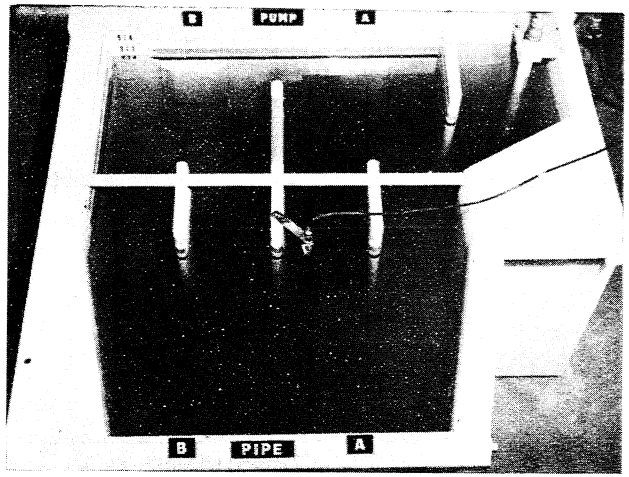

(b) 20 secs. (69 secs. full-scale) after starting injection

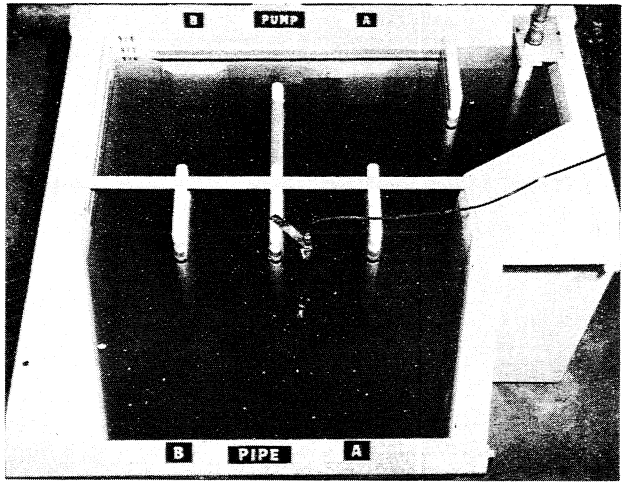

(c) 30 secs. (104 secs. full-scale) after starting injection

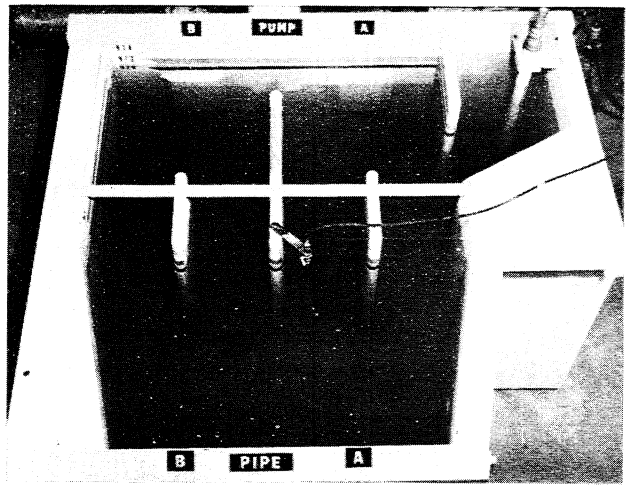

(d) 40 secs. (138 secs. full-scale) after starting injection

Fig. 32 - Dye Simulated Flow Patterns for Acid Injection in the Pump Basin with Pipes A and B Flowing to Pumps A and B.

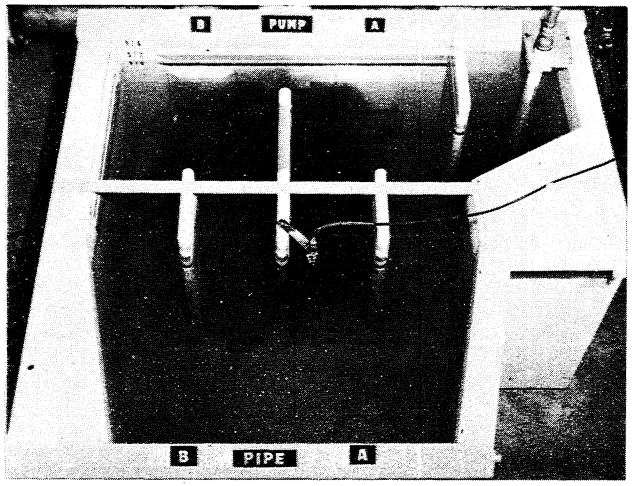

(a) 11 secs. (38 secs. full scale) after starting injection

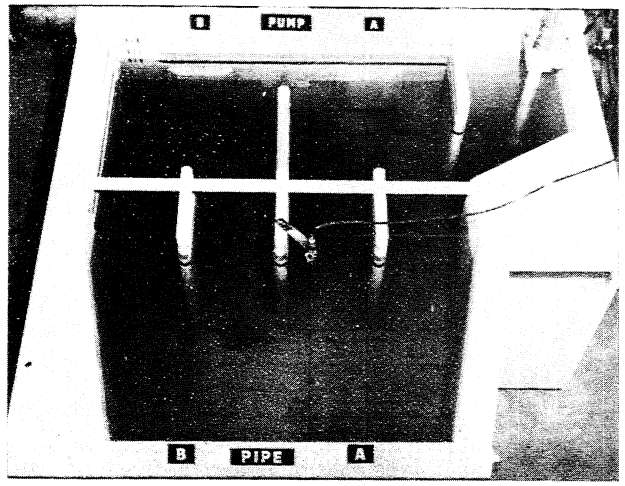

(b) 20 secs. (69 secs. full-scale) after starting injection

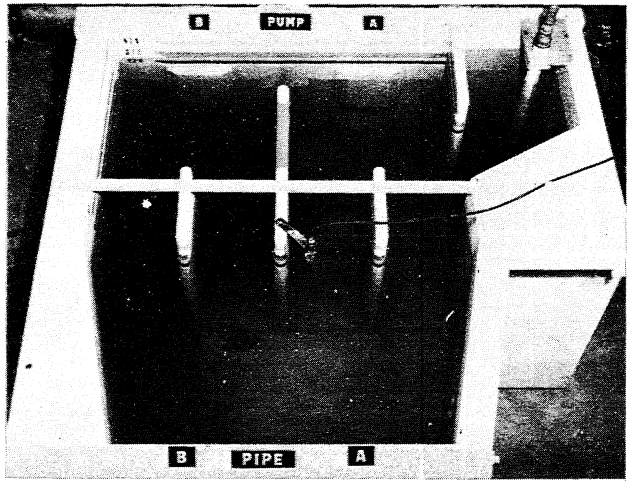

(c) 30 secs. (104 secs. full-scale) after starting injection

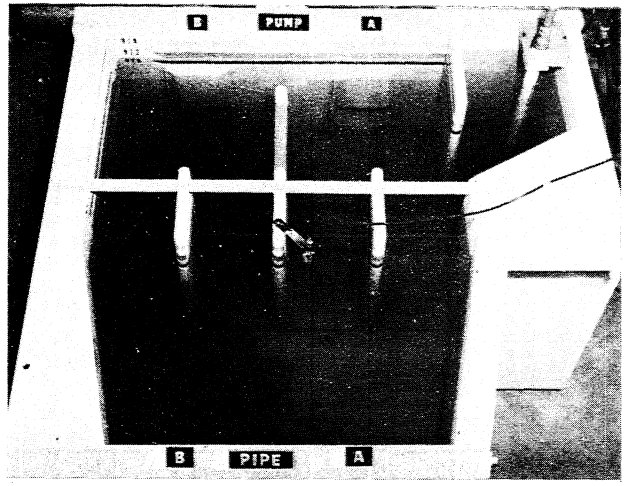

(d) 40 secs. (138 secs. full-scale) after starting injection

Fig. 33 - Dye Simulated Flow Patterns for Acid Injection in the Pump Basin with Pipe A Flowing to Pump B.